ADVANCED MATERIALS
www.advmat.de

Current State and Perspectives of Exfoliated Zeolites

Wieslaw J. Roth, Maksym Opanasenko, Michal Mazur, Barbara Gil, Jiří Čejka,* and Takayoshi Sasaki*

Zeolites are highly efficient industrial catalysts and sorbents with microporous framework structures. Approximately 10% of the frameworks, but eventually all in the long run, have produced both 3D crystals and 2D layers. The latter can be intercalated and expanded like all 2D materials but proved difficult to exfoliate directly into suspensions of monolayers in solution as precursors for unique synthetic opportunities. Successful exfoliations have been reported recently and are overviewed in this perspective article. The discussion highlights 3 primary challenges in this field, namely finding suitable 2D zeolite preparations that exfoliate directly in high yield, proving uniform layer thickness in solution and identifying applications to exploit the unique synthetic capabilities and properties of exfoliated zeolite monolayers. Four zeolites have been confirmed to exfoliate directly into monolayers: 3 with known structures—MWW, MFI, and RWR and one unknown, bifer with a unit cell close to ferrierite. The exfoliation into monolayers is confirmed by the combination of 5–6 characterization techniques including AFM, in situ and in-plane XRD, and microscopies. The promising areas of development are oriented films and membranes, intimately mixed zeolite phases, and hierarchical nanoscale composites with other active species like nanoparticles and clusters that are unfeasible by solid state processes.

1. Introduction

The subject matter of this article concerns direct exfoliation of layered zeolites leading to formation of dispersions of monolayered nanosheets in solution. This is a fundamental expectation for 2D solids but has not been demonstrated with zeolites until recently.

Zeolites are a special class of porous solids with framework structures containing uniform pores and channels. Porous solids are valuable in many industrial processes due to internal void spaces and extended surface areas, which are beneficial in separation and catalytic transformations of organic compounds and inorganic gases.[1,2] The original synthetic porous materials, including various forms of carbon, amorphous silicas, alumina and others were characterized by polydispersity of pore sizes.[3] The emergence of aluminosilicates known as zeolites in the middle of the last century provided crystalline porous solids with periodic structures containing discrete pores and channels below 1 nm. This represented a breakthrough in fundamental research and industrial applications by enabling shape-selectivity, i.e., discrimination of molecules based on size and shape.[4–7] The ensuing research and development resulted in numerous large-scale applications, such as water softening by ion exchange, gas separations, and especially hydrocarbon conversions to enhance production of fuels, lubricants and monomers for polymerization, as well as plethora of other applications. The application of zeolites often leads to environmental benefits.[8,9] Zeolites gave rise to the concept of molecular sieving[4] and influenced the development of other porous materials exemplified by pillared layered solids,[10] mesoporous materials,[11–13] MOFs,[14] MOPs,[15] and related types of frameworks.

The key to uniqueness of zeolites is their framework structure composed of oxygen-sharing tetrahedra, TO_4, with the central T atom such as Si, Al or others.[16,17] They are assembled spontaneously under hydrothermal conditions resulting in different structures providing various pores depending on the composition of the synthesis mixture and other conditions such as temperature and time.[18] The performance and activity of zeolites could be modulated by selecting different structures and compositions to optimize activity toward particular molecules.[19,20] Once produced, zeolite structures were fixed and practically

W. J. Roth, B. Gil
Faculty of Chemistry
Jagiellonian University
Gronostajowa 2, Kraków 30-387, Poland
E-mail: wieslaw.roth@uj.edu.pl

M. Opanasenko, M. Mazur, J. Čejka
Department of Physical and Macromolecular Chemistry
Faculty of Science
Charles University
Hlavova 8, Prague 2 12843, Czech Republic
E-mail: jiri.cejka@natur.cuni.cz

T. Sasaki
Research Center for Materials Nanoarchitectonics (WPI-MANA)
National Institute for Materials Science (NIMS)
1-1 Namiki, Tsukuba, Ibaraki 305-0044, Japan

The ORCID identification number(s) for the author(s) of this article can be found under https://doi.org/10.1002/adma.202307341

DOI: 10.1002/adma.202307341

immutable, resulting in a strategy to obtain as many new zeolite frameworks as possible for diverse uses. The current number of recognized zeolite structures is around 250[21] while about 20 have been commercialized or made technologically ready.[22] Zeolite MWW (MCM-22) patented in 1990 appears to be the last new framework developed for commercial use[23,24] suggesting diminishing returns from the discoveries of new zeolite topologies. New zeolite-based processes are being implemented but they use frameworks known before 1990.[25]

The efforts to discover new zeolite structures produced an unexpected breakthrough that the same framework can form both 3D extended and layered 2D forms.[26–30] Such existence of 3D and 2D forms with the same structure, except for terminations at the surface, is not common so it is significant fundamentally.[31,32] On the practical side, the availability of 2D zeolite allowed circumventing immutability of the traditional 3D zeolite structures and presented the possibility for post-synthesis modifications. Especially valued was the option to expand the structure and increase internal accessibility,[33,34] because the constraints on diffusion and access became invoked as shortcomings-to-be-overcome with the conventional rigid 3D zeolite crystals.[35] For the layered zeolites the examples of intercalation with guest molecules,[36] expansion (swelling) to produce inorganic or organic pillared species,[33,37] layer disordering (delamination)[38] and rearrangements to alternative zeolite structures have been gradually demonstrated.[39–41] These results implied independence of the layers but the ultimate embodiment – exfoliation of the layers, preferably directly, to produce lamellar nanosheets/colloids in solution – remained elusive.[29,42] The fundamental and practical significance of this exfoliation is hard to overstate – the definition of layered materials demands such exfoliation as a proof of the 2D character and in practice allows the use of nanosheets as free gigantic molecules dispersed in a homogeneous liquid phase for combination with other molecules and entities and deposition on or mixing with solids. This presents an open-ended possibility to use the nanosheets as "extended building blocks" for making intimate nanoscale composites and hierarchical materials, many of them unfeasible with the 3D frameworks and even with 2D zeolite solids. The enormous potential of 2D nanosheets dispersed in solution has been evidenced and practiced for a long time with other classes of layered solids and is particularly exemplified by the 2D aluminosilicate counterparts of zeolites, clay minerals.[31,43] The direct formation of suspensions of dispersed zeolite monolayers in solution has not been well documented and remained elusive until recently. The earlier efforts were not direct and relied on pre-expanded, surfactant-swollen layered precursors.[42,44–49] They are overviewed in more detail in the the section 4. The fundamentally expected direct chemical exfoliation resulting in unilamellar nanosheets in solution[50] that could provide versatile substrates for reactions was confirmed first for the zeolite MWW.[51] It was carried out with the reagent that has been commonly used for exfoliation of layered metal oxides, namely tetrabutylammonium hydroxide (TBAOH).[50] This suggests that interlayer chemistry of zeolite nanosheets is not a barrier to exfoliation. Instead, the deciding factor was the preparation method of the layered zeolite, which suggested crystal or layer intergrowths as the most likely primary factors controlling the extent of exfoliation, i.e., the possible yield of dispersed layers in solution. High yield is crucial for meaningful practical exploitation. Since the first publication in 2020 there have been several additional reports with well documented cases of such direct exfoliation.[52–54] They show feasibility for all layered zeolite frameworks and illustrate the requirements for conclusive proving of the genuine monolayered nature of the nanosheet in solution, which is not trivial and requires special approach combining several complementary techniques.

The present perspective article reviews the advances and discusses the fundamentals peculiar to such systems and emerging possibilities for development of zeolite materials in new directions, including application beyond those demonstrated and practiced so far. In particular, as mentioned above, the exfoliation enables unconstrained combination of zeolite layers with desired functional components to produce nanoscale hybrids and hierarchical structures that are unimaginable with the 3D frameworks. The development of zeolite nanosheets in solution showed insights that also illustrate challenges and possible shortcomings that may have to be overcome. It is hoped that this perspective will initiate a roadmap for the development of exfoliated zeolites as unique materials that can extend the possibilities of using 2D solids by providing nanosheets with pores and strong acid centers.

2. Explanation of the Nomenclature

The question of nomenclature arises because there are two basic terms describing separation of layers in 2D solids: delamination and exfoliation. Specific definitions have been proposed for differentiation between them but there are discrepancies between different literature sources including incompatible or opposite meanings.[32,53,55,56] These terms are not applied consistently in the literature and have been used interchangeably in diverse situations for both liquid and solid systems.[32,57] There have been proposals for strict and uniform usage and differentiation between these two terms[55] but they face problems with the past, i.e., application and sorting out the historical, already published data, and with the future, buy-in and meaningful compliance among scientists, which if agreed in principle may take time. The problem at hand is naming of the zeolite systems reviewed herein, i.e., stable dispersions of monolayer nanosheets in solution.[51,53,55] Exfoliation is the most appropriate and convenient term to apply for several reasons starting with the need for differentiation from delamination and delaminated zeolites. The latter concepts are already firmly established in reference to disorganized layers as final solids with particular interest for catalysis.[57–59] Zeolite delamination has not been concerned explicitly with the dispersion into monolayers in solution and there is no evidence that the latter have played any but a minor role in it, if at all.[60,61] Aside from this practical reason, the term exfoliation is already often used to describe the process of transforming 2D solids to obtain monolayers in solution[62] and in that sense has been reviewed in the seminal review as liquid exfoliation.[32] This understanding is supported by the definition of exfoliation provided in the Glossary of Clay Science, which says:[56] "exfoliation involves a degree of separation of the layers of a host structure where units, either individual layers or stacking of several layers, are isotropically dispersed (freely oriented and independent) in a solvent or polymer matrix." For comparison, in the Glossary delamination is described as "layer-separation process between

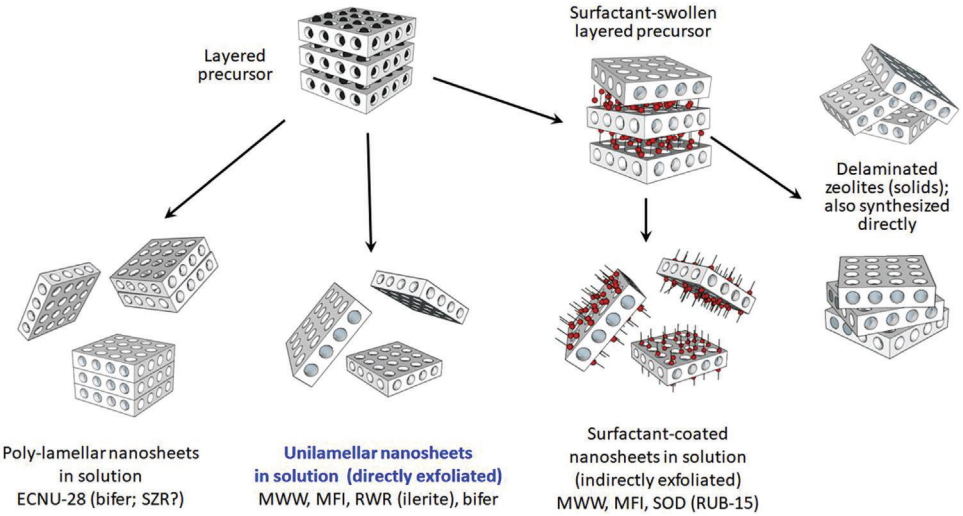

Figure 1. Basic types of solution dispersions of layered precursors with examples of reported materials. The systems discussed in this article are in the middle.

the planar faces of adjacent layers of a particle (...) whereby intercalation occurs with the introduction of guest material and the stacking of layers remains." This definition is consistent with delaminated zeolites in the as-synthesized form, which usually contain guest species between layers, inorganic, organic, or both.[61,63,64] The organics are removed by calcination to afford the final (delaminated) solid.[38] By adding the descriptor "synthesized directly" this definition can encompass the materials obtained in one-pot hydrothermal synthesis like MCM-56[65] or MWW zeolite nanosheets prepared via one-step syntheses.[59] In summary, the adoption of exfoliation and delamination as advocated above is consistent with the prevailing usage of the former and differentiates from the very popular class of delaminated zeolites. To avoid ambiguities, we also adopted full descriptions like "directly exfoliated unilamellar nanosheets in solution" to provide precise meaning to the referenced materials. Direct means that exfoliation can occur spontaneously upon contacting the layered solid with the exfoliation medium, with optional mild agitation. It is different from exfoliation attempted by pre-expansion with surfactants followed by extrusion with polymers, extraction and purification.[44,45] 'In solution' refers to the homogeneous liquid phase, without specifying 'a solution' or 'sol'. It is also needed to differentiate from "exfoliated layers" recovered as solids, pure or in mixtures from these solutions. Finally, unilamellar emphasized the absence or minimization of multilayered particles, which for each first case is rigorously verified. The alternatives are polydisperse suspensions shown in **Figure 1**.[66] This terminology with longer descriptive phrases may look cumbersome and like unnecessary repetition but, in our opinion, provides clarity and eliminates ambiguity in comparison to other processes and systems involving 2D materials. It is based on precisely defined outcome not a particular name, which can be understood in various ways. An alternative precise concept of 1D dissolution for exfoliation into monolayers has been proposed recently but it is novel and will need time for validation and wider acceptance.[55]

Zeolites with a known framework structure are represented by capital 3-letter codes like MWW and MFI, while the structure of bifer is unknown so it is written in small letters. MCM-56 and MCM-22 represent various synthetic forms of the zeolite MWW.

3. Prior Attempts at Zeolite Exfoliation into Monolayers in Solution Especially with Surfactant Pre-Expanded Precursors

Complete separation of 2D solids into individual layers has both fundamental and practical significance. Arguably, the recent reports of direct exfoliation of layered zeolites[51–54] producing solutions with monolayer nanosheets, represent a watershed, providing zeolite layers with maximally exposed surfaces. Prior to that, the concepts of delamination and delaminated zeolites, referring to the efforts of layer separation, were focused on the isolation and characterization of the final solids, which did not allow judging the extent of layer separation.[38,67] In contrast, liquid exfoliation,[32] denoting dispersion of monolayers by and into a liquid medium provides complete layer separation as a distinct stage and can be a possible benchmark for assessing both the effectiveness of layer separation and product quality, obtained by other delamination procedures. This role can be useful because of the lack of an objective quantitative method of estimating the extent or quality of delamination in a solid state. On the practical side, successful liquid exfoliation provides nanosheets in solution as reagents for unconstrained combinations with compositions of choice, as underscored by the studies on graphene and related systems.[68–71]

It is reasonable to assume that in the majority of reported procedures of zeolite delamination the presence or role of layers being exfoliated into a liquid phase was minimal. There was also no effort to explicitly exploit, prove or invoke this crucial stage. Starting in 2011,[44] several studies did report preparation and usage of dispersed zeolite monolayers in solution but they were not obtained directly. The layered zeolite samples were expanded with

surfactants, during or post-synthesis, and processed via multistep methods. For reasons elaborated below their practical impact was limited.

It is helpful to point out that examples of successful direct exfoliation of layered zeolites indicate the crucial role of the nature of the sample as determined by the procedure of its synthesis, namely gel composition and conditions of synthesis. Given a suitable sample, presumed to have low level of intergrowths, the finding of reagents and conditions for exfoliation appears to be routine. In contrast, the prior studies to separate and disorganize zeolite layers were focused on finding reagents and treatments for layered zeolite samples at hand, which could have been poorly exfoliable from the outset. There were separate efforts to design direct syntheses for delaminated zeolites, but they were also focused on the final solid product.[59] There are also classical approaches used for the preparation of layers of other classes of 2D materials (carbons, transition metal oxides, chalcogenides, etc.) but they are not applicable for zeolites. Examples include bottom-up techniques based on vapor phase deposition utilized for 2D carbon and transition metal compounds,[72] or micromechanical cleavage and chemical oxidation methods for graphene and its derivatives.[73,74]

Layered zeolite forms have been obtained with ≈10% of the known frameworks and new examples are being added incrementally.[75] Syntheses by design have been also reported, for example with bifunctional templates for single layers[76,77] and the top-down approach denoted ADOR.[40,78] There have been reports of disordered single-layered materials synthesized directly but the layers were usually intergrown, which was not favorable for exfoliation into solution.[76,77]

The concept of delaminated zeolites[38] gave rise to many investigations based on preswelling with surfactants[33] followed by the application of stimuli or additional reagents to separate the layers. In comparison to direct exfoliation reviewed in this article those techniques require several steps and in most cases were focused on final solids. The possible intermediate exfoliated nanosheets in solutions, where in most cases were unlikely to form or at best at negligible amounts. The exception was the study in 2011 involving layered precursors of MWW and MFI with layers separated by surfactants that were incorporated either post synthesis or as templates during preparation, respectively.[44] These surfactant-swollen composites, expanded by ≈2.5–3 nm, were combined with polymers in a twin-screw extruder, mixed with appropriate solvent like toluene, and purified by density gradient centrifugation to remove multilayered particles. The obtained supernatant contained exfoliated nanosheets, coated with surfactants, which could be an obstacle to interaction in subsequent syntheses. Nonetheless, it was the first successful demonstration of exfoliated zeolite monolayers in solution.[44] The exfoliation was proven by the combination of diffraction (XRD, ED) and microscopy techniques (HRTEM, AFM) validating the structure of the MFI and MWW layers and confirming uniform thickness after purification. The verification of single layers in solution did not include techniques like SAXS, in situ and in-plane XRD, which played an important role in the validated directly exfoliated layers (vide supra).[51,52,54] The dispersed nanosheets were used to fabricate oriented zeolite films, which after repair to eliminate defects showed effective gas separation of small molecules.[44,45,48] This work was notable by demonstrating zeolite exfoliation and its effectiveness for the fabrication of oriented zeolite films but its practical side was limited. The multistep strategy based on a sequence of interlayer expansion, melt blending using a special equipment, dissolution, and purification has not been conducive to entice broader studies and applicability. Melt blending itself is a well-known, noncostly procedure used for exfoliation of inorganic layered solids.[79] In the paper on zeolite exfoliation by melt blending, a relatively simple system was used: a corotating twin screw extruder with a recirculation channel utilized under inert atmosphere.[44] However, in comparison to anticipated and subsequently demonstrated direct exfoliation methods rewieved herein, the disadvantages of the multistep procedure combined with elevated temperatures (200 °C), low yield (5%, later increased to 10%[80]), and layer covering with long surfactant chains presented serious obstacles.

This initial exfoliation approach based on preexpansion of layered zeolites was continued with further refining and improvements. One of them was the use of different polymers such as polystyrene, polybutadiene, polylactic acid, and polyvinylpyrrolidone for dispersion of swollen MWW materials.[46,79,81] A hydroxyl-terminated polybutadiene (HTPB) was applied with purely siliceous MWW also preswollen with hexadecyltrimethylammonium cation, HDTMA.[82] For layer purification chemical treatments with either acid as a single component or in the mixture of sulfuric acid and hydrogen peroxide (the so-called piranha solution) have been applied to decrease the fraction of organics in the final material.[83] From the economic standpoint, zeolite film and membrane applications can tolerate significant cost and labor increases associated with fabrication but the concern for sufficient quantity and concentration for potential applications as medium- and large-scale processes remained a major issue.[84] An example of yield enhancement in the method involving melt blending was the combined purification process that included the removal of polymer residues by density gradient centrifugation and the exclusion of oligo-layered aggregates by rate-zonal centrifugation in a multicomponent solvent system. It allowed to increase the yield of nanosheets from 5 to 10%.[80]

The use of melt blending exemplifies application of extra force (mechanical) in addition to chemical interaction to enhance layer separation. It is a common engineering tool, but it is hard to pinpoint if and how it seems to be effective. It is possible that the major effect is mechanical fracturing, resulting in layer fragments separating from the rest. The direct exfoliation of zeolites reported since 2020, exemplified by ilerite and MWW, have been accomplished without and with stirring, respectively. The applied stirring is not viewed as a surce of additional mechanical force but simply to accelerate kinetics, which otherwise would have to rely on slow diffusion. Examples of additional mechanical stress can be found with all layered materials, including those more chemically flexible than zeolites, such as metal-organic frameworks[85] and covalent organic frameworks.[86] Besides affecting the layers, the application of shear forces (e.g., by rotating screws) or acoustic cavitation (by sonication) to aid the exfoliation can also improve the mobility of molecules (solvent, surfactant) in the interlayer space, thus increasing the exfoliation efficiency.[79,87] On the other hand, the recent successful exfoliation of zeolites indicates that with suitable physical and chemical circumstances, namely

crystals without intergrowth and appropriate medium, the need for mechanical stimuli diminishes.

Although zeolite crystals are typically prepared at pH near 12 and higher, still when separated from the synthesis mixture they may be susceptible to degradation under basic conditions. A matter of some concern in separating zeolite layers by delamination and swelling post-synthesis has been the strong basicity of the reaction media and the possibility for negative effect on the integrity of zeolite layers, loss of crystallinity, defect generation and possible formation of undesired phases. Reported solutions included swelling at room temperature "with layer preservation,"[88] using lower pH = 9 by swelling in the presence of fluoride and chloride anions,[64,89] and using water-soluble metal salts of Al or Zn under acidic conditions (pH = 1–3).[58,63] These studies demonstrated the possibility of separating or disorganizing zeolite layers in a solid but did not show nor sought the formation of exfoliated nanosheets in a liquid phase. There is a caveat because the effectiveness of expansion/intercalation of layered zeolites under mild conditions diminishes with increasing Al content. The latter determines acid site concentration and overall activity and in many catalytic processes its maximization is desired.[61,90] Based on the analysis of published data[91] it was shown that swelling of MWW at high pH and elevated temperature, which may result in desilication and partial framework degradation, did not diminish catalytic activity.[90] Some literature reports show the use of multilayered aggregates, which can be obtained by using small zeolite seeds for a bottom-up membrane growth.[92,93] This method is not based on exfoliation but provides films consisting of layers of about 5 nm thickness (larger than for a single layer) that are not aggregated or intergrown, and thus can be used with almost no limitations for the preparation of ultraselective membranes.[92] Other examples of tolerance for oligo-layers include MFI systems treated with piranha solutions,[83] hydrogen peroxide decomposition at elevated temperature between MWW layers (up to 180 °C) in a microwave,[94] and simple treatment of MWW with ethanolamine. The last method produced thickness reduction and sufficient uniformity of nanolayer for deposition on paper macroscopic objects via dip-coating for their protection against acidification, aging, and oxidation.[95]

Summarizing, prior to the recent reports of direct exfoliation of layered zeolite affording unilamellar nanosheets in solution, this desired outcome was possible only through low yield multistep processing producing layers coated with surfactants. This enabled valuable applications for membrane fabrication but was impractical for more general uses in syntheses. What was not recognized was that quality of the layered zeolite might be crucial for direct high yield exfoliation into monolayers. As shown below, such exfoliation of layered zeolites into unilamellar nanosheets in a homogeneous liquid phase can be achieved by simple soft-chemical treatments with appropriate solid samples. An illustrative example is provided by the first case, zeolite MWW, which has been exfoliated only as the MCM-56 preparation.[51] Historically, the most studied form for delamination was the multilayered precursor, MCM-22P, which so far has not shown dispersion into monolayers in solution by the same procedure as MCM-56.[44,49] This resistance to direct exfoliation may be prevented for fundamental reasons but maybe an exfoliable MCM-22P form is still to be found/prepared.

4. Proving Monolayered Nature of Zeolite Nanosheets in Solution

The procedure for direct exfoliation of layered zeolites into monolayer nanosheets in solution involves mixing solids with the dispersing solution followed by centrifugation to sediment larger or multilayered particles. The resulting solutions often appear colloidal-like with translucence/opalescence and are stable without visible sedimentation for long periods of time (weeks and months). This does not prove exfoliation into monolayers and special characterization is necessary to rule out the presence of multilayered particles. Preliminary identification such as powder XRD can be carried out by isolating solids by flocculation but more elaborate techniques are needed to confirm the presence of truly unilamellar nanosheets in solution. The discussion will focus first on the methodology for proving monolayers in solution and determining their structure, while the synthetic aspects are described in the next section. This proving of the presence of monolayers in solution and characterization of their structure is based on a protocol combining the following methods:[51,96]

i. SAXS for measuring interlayer d-spacing in solution,
ii. in situ XRD confirming mono-dispersity and structure of the layers in solution,
iii. AFM to show distribution of layer thicknesses,
iv. in-plane XRD to determine the planar unit cell,
v. X-ray diffraction, TEM, and ED to characterize layer structure, and
vi. flocculation reaction, e.g., with a surfactant, to show formation of multilayered composites with alternating inorganic and surfactant layers with specific d-spacings.

The first 3 methods provide basic, close to complete description of the layers in solution. The remaining methods focus on structure and corroboration of the initial results. Additional supplementary techniques can be applied and, needless to say, self-consistency of the results proves successful preparation of zeolite monolayers in solution.

To date, direct exfoliation into monolayers in solution has been proven with four zeolites. Basic structural details and applied characterization methods are summarized in **Table 1**. The confirmed exfoliated zeolites are: MCM-56 with the MWW topology,[51] bifer with unknown structure that may be related to ferrierite because of analogous unit cell and synthesis from a gel producing ferrierite layers,[52] MFI—one of the two most important zeolites with ≈0.5 nm pores perpendicular to the layers,[54] and ilerite, a layered silicate that is a precursor to zeolite RWR.[53] The extension to other frameworks depends on finding suitable preparations that are conducive to exfoliation. A detailed review of each characterization method is presented below. The first three zeolites were exfoliated with TBAOH. Ilerite was exfoliated with meglumine (*N*-methyl-D-glucamine) under milder conditions, which may result in differences between products from these two approaches. A treatment of ilerite with TBAOH did not result in exfoliation.[53]

The first method, small angle X-ray scattering (SAXS) can reveal characteristic distances in partially ordered systems.[97] It has been carried out for the MWW (MCM-56) samples treated with aqueous solutions of TBAOH at different concentrations.[51] A

Table 1. Summary of the methods used to prove direct zeolite exfoliations into solutions of monolayer nanosheets. Sodalite precursor exfoliated via pre-expansion with surfactants is included for comparison.

	MWW	Bifer (unconfirmed structure)	MFI	Ilerite (RWR)	RUB-15 (sodalite), via HDTMA swelling)
Layer thickness [nm]					
Crystal	2.4	1.9	3.0 (unit cell 2.0)	0.74	0.8
Exfoliated as-made calcined	2.5	2.1	3.6	1.38	1.14
	2.3	1.8	2.8	N/A	0.74
Characterization tool					
SAXS	+	No	No	+	No
In situ XRD	+	+	No	No	No
AFM	Statistic	Statistic	Statistic	Individual	Individual
In-plane XRD	+	+	+	No	No
TEM/ED	+	+	+	+	+
Nanosheet solution + HDTMA reaction	+	+	+	No	No
Film by filtration	+	+	+	+	+

series of basal peaks were detected, giving largely expanded interlayer spacing of 5.3–6.2 nm (**Figure 2**) as a function of the TBAOH concentration. These values indicate the interlayer expansion by 2.8–3.7 nm, which is much larger than the size of TBA^+ ion, ≈1 nm. Thus, this behavior can be understood in terms of unique interactions, called osmotic swelling, which has been reported for ion-exchangeable layered host compounds including clay minerals, layered transition metal oxides and layered double hydroxides (LDHs).[98–103]

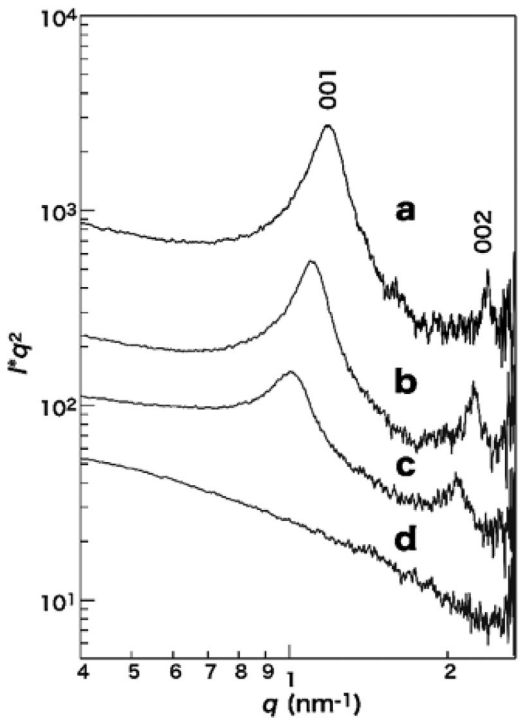

Figure 2. SAXS profiles for MWW samples in aqueous TBAOH solutions at different concentrations (10, 8, 6 and 4 wt% from a–d). A solution volume to solid weight ratio is 54 cm^3 g^{-1}. The interlayer distance observed is 5.3, 5.7, and 6.2 nm for a–c, while no Bragg peak is detected for d (4% TBAOH). Reproduced under terms of the CC-BY license.[51] Copyright 2020, The Authors, published by American Association for the Advancement of Science.

This phenomenon reflects enormous hydration-driven swelling in smectite clay minerals that has been studied from as early as 1950s.[98,99] When alkali metal ions such as Li^+ and Na^+ with high hydration energy are incorporated into the clay interlayer gallery, a large volume of water is permeated to produce a gel-like sample. The interlayer distance is largely expanded to over 100 nm. It has long been believed that this unique reaction is peculiar to a special class of clay minerals. However, in 1998 it was reported that a polycrystalline layered titanate underwent massive osmotic swelling upon contacting with aqueous TBAOH solutions.[100] More recently, accordion-like swelling of platelet crystals of layered metal oxides such as titanates and perovskites was observed directly under optical microscope.[102,103] Unidirectional ≈100-folds expansion of the crystals into long string-like objects took place in a few seconds. Surprisingly, thousands of layers are stably held parallel together, having a large volume of the solutions between them, up to ≈100 nm in thickness. The swollen crystals can reversibly go back to original platelets upon some stimulus, e.g., change in electrolyte concentration or pH. On the other hand, Davidson et al. recently reported that highly swollen accordion-like crystals of smectite clays are kinetically stable.[104] Full understanding of this intriguing phenomenon needs to await further studies. This massive osmotic swelling is induced in various layered metal oxides with a range of amines and organoammonium ions. The degree of interlayer expansion is not dependent on the chemical species but is determined solely by their concentration. The swelling tends to be stable with polar and smaller amines while opposite with large symmetrical species.[101] On the other hand, LDHs, anionic clays, were found to show similar swelling in formamide. The basal spacing as large as 8 nm was observed at a large excess of formamide.[105]

The degree of swelling of the layered materials above including layered zeolites can be controlled by the concentration of electrolyte solutions. In general, the swelling is enhanced with decreasing concentration. In the case of MCM-56 zeolites with

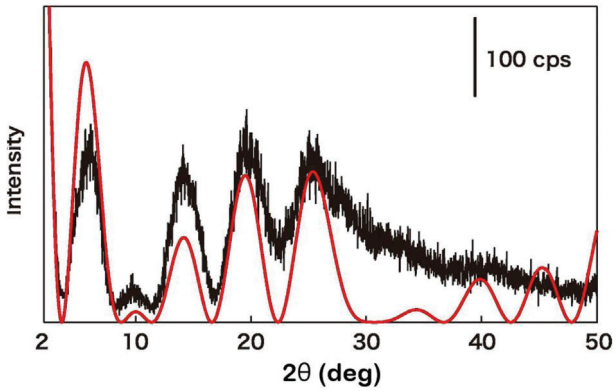

Figure 3. In situ XRD data of the glue-like sample recovered from the colloidal suspension by the high-speed centrifugation (black line) and the square of the structure factor F (red line) calculated based on the MWW structure. Reproduced under terms of the CC-BY license.[51] Copyright 2020, The Authors, published by American Association for the Advancement of Science.

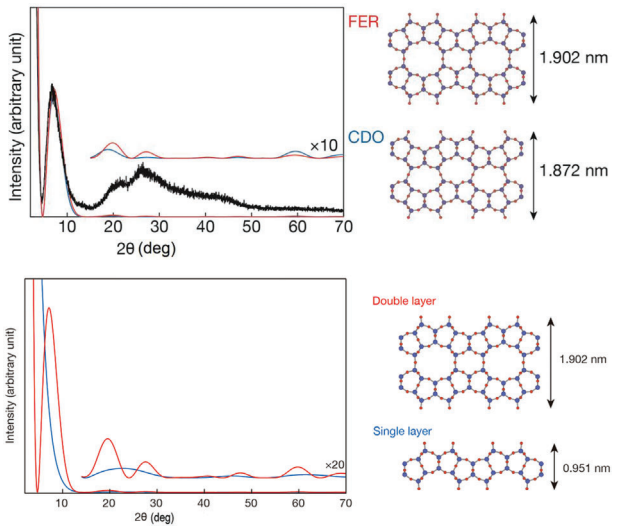

Figure 4. Comparison of in situ XRD results for bifer layers with calculated profiles for doubled layers with FER and CDO structure and single fer layer. Reproduced under terms of the CC-BY license.[52] Copyright 2021, The Authors, published by The American Chemical Society.

MWW layers, the basal peaks shifted toward the smaller angle side with lowering of the TBAOH concentration as shown in Figure 2a–c. The SAXS data presented in Figure 2 represent the hydration-driven expansion (swelling) process of the layered zeolite MWW, which eventually ends up with separation into unilamellar nanosheets. In these experiments the swollen samples of layered zeolites were collected via centrifugation and a glue-like sedimentation was produced and subjected to SAXS analysis. The SAXS data were recorded for the sample, which was not exfoliated yet (on its way to it). As can be seen, the interlayer separation progressively expanded. This is the swelling process where the layered structure is maintained, and thus a nematic phase of exfoliated nanosheets is not formed. The observed shift clearly indicates the progress of swelling. It is expected that the larger the interlayer distance, the weaker the interaction between the layers through the interlayer fluid. Then at the massive swelling the layers fall apart, facilitated by applying the external force like mechanical agitation. In practice, the basal peaks disappeared at a threshold concentration (Figure 2d), suggesting the loss of the regular layered structure, namely the total exfoliation. A recent review by Breu explains this phenomenon as '1D dissolution.'[55]

The samples at low TBAOH concentrations became colloidal suspensions of layers with translucent appearance. The dispersed layers were recovered by high-speed centrifugation as glue-like substances and subjected to X-ray diffraction (XRD) measurements at high relative humidity to suppress the drying. The illustration of the unique set up for this measurement was provided in the Supporting Information in reference [51], This in situ XRD analysis provides important information about the colloidal state of the zeolite samples. **Figure 3** depicts such typical data for the MWW sample, showing a broad and oscillating profile peculiar to the material. Importantly, this pattern is closely matched to the calculated profile as square of the structure factor based on the MWW layer topology, meaning that the layers scatter X-ray individually. In addition, no basal peaks were observed, indicating the absence of a regular stacked structure. All these results clearly prove that the multilayered MWW structure was disintegrated into colloidal single layers dispersed in aqueous solutions. Similar analysis has been reported for various layered materials such as clay minerals, layered transition metal oxides and LDHs.[106–109]

The in situ XRD technique is useful not only for confirming total exfoliation but can also help with identifying more complicated or not fully known structure of the nanosheets. This is illustrated by the material denoted bifer, which was obtained upon modifying the synthesis of the layered zeolite ZSM-55 by substituting boron by aluminum. The layers in ZSM-55 are ≈0.9 nm thick[30] and are designated fer because they have the topology of the zeolite ferrierite (FER) but can produce 2 different structures upon topotactic condensation: FER upon reflection in mirror planes and CDO through translation.[41] The product from the modified sythesis was clearly different from ZSM-55 based on XRD, but was found by in- plane XRD to have a rectangular unit cell (b and c axes) similar to fer (see Table 1). The layer thickness seemed to be doubled in comparison to fer leading to the designation bifer. The structure of bifer was unknown but for simulations such as in situ XRD a model was needed. The structures CDO and FER were considered. The simulation of theoretical in situ XRD patterns was carried out for a single fer layer and double-layered FER and CDO structures, see **Figure 4**. The observed experimental wavy pattern layer is vastly different from the calculated profile for a single fer layer and clearly not acceptable as a possibility. In contrast, the double-layered models gave very similar profiles resembling the experimental one, proving doubled layer thickness in bifer. Unambiguous differentiation between FER and CDO was not possible. As a new development concerning the identity of bifer, a recent publication reported layered material ECNU-28, which shows XRD pattern very similar to that of bifer.[66] The authors argue that the patterns are different and propose the SZR topology for ECNU-28. Questions can be raised about validity of this conclusion and the structure determination. This will be discussed as a separate topic below.

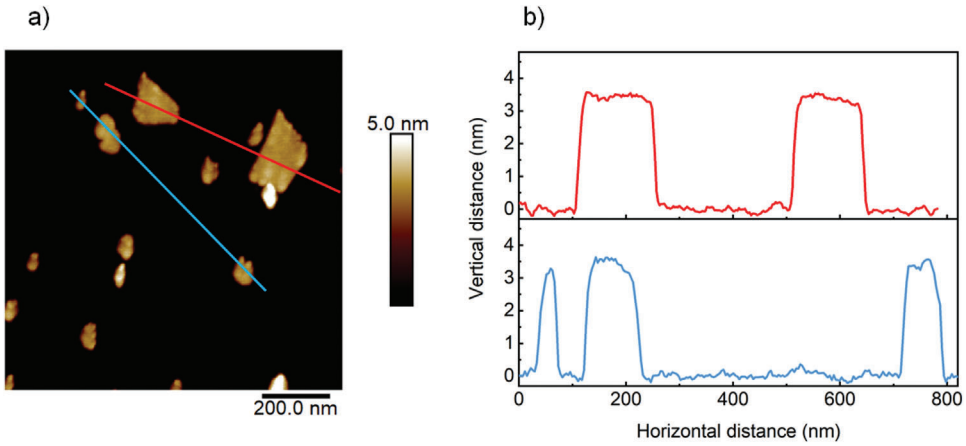

Figure 5. Illustrative AFM results – for zeolite MFI layers. Reproduced under terms of the CC-BY license.[54] Copyright 2023, The Authors, published by The Royal Society of Chemistry.

AFM is one of the most powerful tools to characterize nanosheets with ultrathin 2D morphology.[110] Generally, colloidal nanosheets are deposited on an atomically flat support, e.g., Si wafer, and probed by cantilever with an appropriate spring constant. The deposition from the suspension is facilitated on surfaces covered with polycations such as polyethyleneimine (PEI). Minimizing overlap of nanosheets is desirable and is possible by appropriate dilution, e.g., 100 times with 1% w/w nanosheet solutions. Measurement of the elevation above the background is performed for individual nanosheet but it is preferred to carry out a more complete statistical distribution of heights over entire viewing area and in several regions (see Table 1).

As exemplified by a typical image for the MFI zeolite nanosheets (**Figure 5**), many 2D objects are detected. The objects have a very flat terrace with a unique height, revealing the molecularly thin feature with a high aspect ratio.

AFM data for zeolites MWW, MFI, and bifer showed prevailing elevation (layer thickness) approaching 90% and more of the population, corresponding to monolayers with the average thickness of 2.5, 3.6, and 2.1 nm, respectively. Ilerite layer thickness was 1.38 nm. These values are a few tens of a nanometer greater than the crystallographic unit cell of the corresponding 3D solids, i.e., 2.5, 3.0, and 1.9 nm. The difference is explained by hydration of the layer surfaces, which is commonly observed for various nanosheets.[111] Lateral sizes are variable reaching widths of the order of 100 nm. This implies nanosheet fragmentation, which has not been examined in detail and may be relevant with time or require optimization for applications. Particles with a thickness above the apparent monolayer values constitute roughly 10% or less of the deposited materials and can arise from incidental overlap during deposition, association is solution or simply multilayer "impurities" present from the beginning. The AFM results indicate that the obtained suspensions can be considered monodisperse with regard to the nanosheet thickness and contain essentially monolayers only. There is a small chance that particles deposited on the support are not fully representative of the content of the suspension so further validation with other methods is desirable, especially when dealing with a given system for the first time. In situ XRD described above can be this validating characterization tool.

Patterns obtained by the in-plane XRD technique contain only in-plane reflections allowing determination of the planar unit cell dimensions of the nanosheets. In principle, this information is contained in powder XRDs but it may be difficult or impossible to extract due to low quality, peak overlap, unassignable scattering related to thin layers and the impossibility of indexing. The examined nanosheets are deposited on a Si substrate and incident X-ray is scanned parallel to it. This can produce sharp peaks, especially when collected with synchrotron radiation (**Figure 6**), and upon indexing 2D unit cell dimensions can be obtained. In the case of MWW, MFI, and bifer, all in-plane peaks were indexed proving purity and consistency with the corresponding 3D framework model (known for the first two). The patterns in Figure 6 show relatively simple in-plane XRD with all peaks identified, contrasted by complicated powder XRD pattern with some broad and unidentified peaks. The application of in-plane XRD is particularly beneficial with nanosheets of unknown structure like in

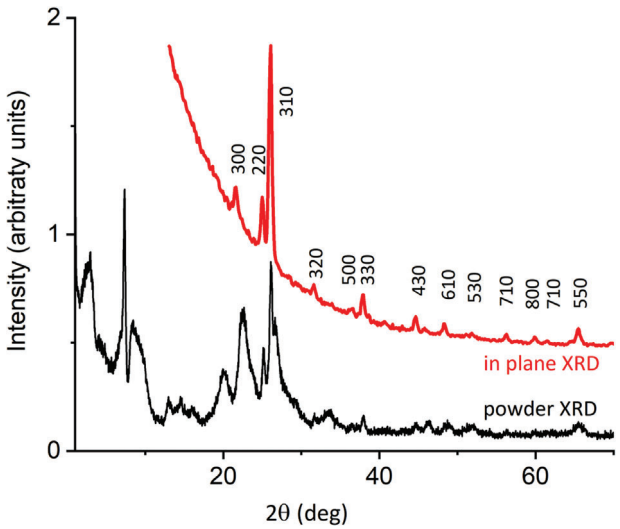

Figure 6. In-plane XRD for the MWW layers compared with the powder pattern. Reproduced under terms of the CC-BY license.[52] Copyright 2021, The Authors, published by The American Chemical Society.

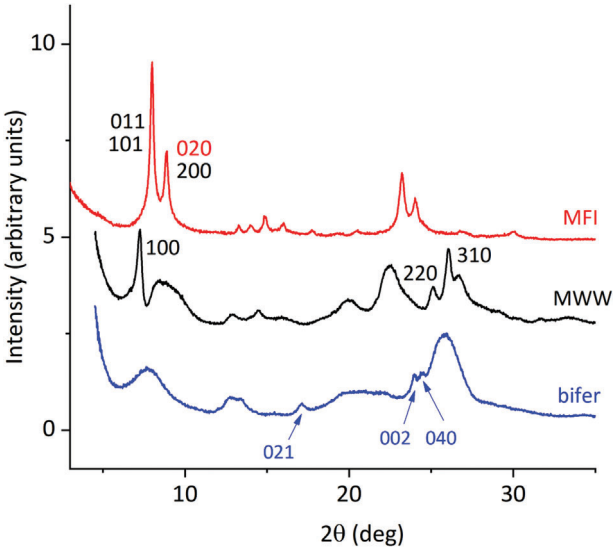

Figure 7. XRD patterns of layered MWW, bifer, and MFI powders.

the case of bifer layers. Thanks to in-plane XRD the planar unit cell was determined to be similar to fer. The structure was not solved but with known unit cell dimensions, reasonable models like FER and CDO could be proposed for simulations.

The combined results from in-plane XRD and AFM provide reliable information about crystallographic unit cell dimensions of nanosheets. They allow correlation with expected values for 3D frameworks and confirmation of the likely internal structure of the layers. In situ XRD and AFM can confirm monolayered nature of the nanosheets in solution.

The primary tool for identifying and characterizing zeolite nanosheets is powder X-ray diffraction (XRD). The XRD patterns for the nanosheets in the solid state and 3D microcrystals are different but are expected to contain common distinct in-plane reflections.[112] The nanosheet XRDs usually contain broad peaks or bands that are hard to assign or identify, and may include non-Bragg scattering like with MCM-56 and bifer (**Figure 7**).[65,113] The XRD pattern of MWW nanosheets is one of the most analyzed examples, including theoretical simulation, which match experimental profiles.[44,113–115] The pattern contains relatively sharp peaks due to 100, 200, 220, and 310 reflections and a broad band without a valley between 8 and 10° 2θ (CuKα radiation everywhere, except when specified otherwise). The band is instead of 101 and 102 reflections in the 3D structure, at 8 and 10° 2θ, respectively, indicating absence of order in the 3rd dimension. Appearance of the valley between 8 and 10° 2θ is interpreted as partial ordering of the layers in 3D proportional to the depth of this valley.[65] Both the starting MCM-56 and the exfoliated nanosheets after isolation as a powder exhibit disordered patterns. The situation is similar with the bifer layers, i.e., the original and exfoliated nanosheets show similar XRD pattern, except for the interlayer $h00$ reflections, which are more distinct with the latter.[52] The intralayer $0kl$ peaks are identified based on the in-plane XRD. The majority of distinct peaks in the XRD of MFI are in-plane so the difference between the patterns for nanosheets and 3D crystals is not pronounced.[54] Summarizing, the XRD patterns of exfoliated nanosheets after isolation confirm their basic structure as it was before the treatments. The reduction of XRD pattern quality when going from 3D to 2D frameworks usually precludes direct structure solution. This motivates additional verification by ED and TEM.

Electron diffraction and TEM complement the powder XRD and other techniques and provide further details about the structure and quality of the layers. The anisotropic shape of the layers favors planar deposition on the support, frequently allowing "top views" for examination. The studies of MWW, MFI, and bifer show periodic patterns extending tens of nanometers confirming framework preservation.[51,52,54] A compilation of selected images is presented in **Figure 8**. Electron diffraction of exfoliated ilerite revealed an interesting situation of lowered symmetry of the layers in comparison to the 3D framework.[53] The latter is centrosymmetric and showed specific systematic absences in the ED pattern. The center of symmetry arises when the layers are stacked in the crystal but is removed upon exfoliation, resulting in disappearance of the conditions for extinction. The resultant pattern has more visible spots allowing distinguishing 3D zeolites from exfoliated monolayers. This is applicable to specific cases where the 3D and 2D forms may exhibit different symmetry but if so, can be used as additional proof confirming exfoliation into monolayers.

TEM imaging is valuable for quality appraisal and visualization of pores. All exfoliated types of nanosheets were studied by TEM. An interesting case arose with the mixture of MWW and bifer (examined as a silica pillared sample). Despite the 0.5 nm thickness difference it was not possible to distinguish unambiguously between them. In some edged-on views the pores were sufficiently distinct to allow clear recognition of bifer based on the density of pores, which for FER and CDO could be similar.

Nanosheets in solution can be confirmed by chemical means by flocculation with cations, especially surfactants. The precipitated solids show XRD patterns with relatively high intensity and well-defined basal spacings allowing estimation of interlayer spacings. The reaction with excess of a cationic surfactant like HDTMA (hexadecyltrimethylammonium) stands out as particularly illustrative, facile, and useful in providing vital information, including yield estimate of the dispersed nanosheets. The mixing of exfoliated layer solutions with surfactants results in immediate formation of a white solid, which is analogous to the layered zeolite swollen with HDTMA-OH. It is generally a multilayered composite with alternating zeolite layers and surfactant bilayers (typically 2.5–3 nm thick with HDTMA, see Figure 8, top right). The three nanosheets, MWW, MFI, bifer, showed XRD with peaks positions matching those in equivalent materials obtained by swelling of the layered precursors. This also indicates the prevailing monolayer nature of the nanosheets in solution. Moreover, the intensities of basal peaks appeared augmented in comparison to the intralayer reflections suggesting greater extent and uniformity of interlayer separation than in the swollen ones. A possible reason is that upon swelling of the solid not all layers become separated, e.g., due to intergrowth, while with nanosheets in solution the initial state is total separation. The reaction of solutions with exfoliated nanosheets with HDTMA can be used for a quick (visual) assessment of the amounts of monolayers in a given preparation. The flocculation is also useful for verifying exfoliation with subsequent samples since it is not practical to validate all solutions by the advanced physical techniques

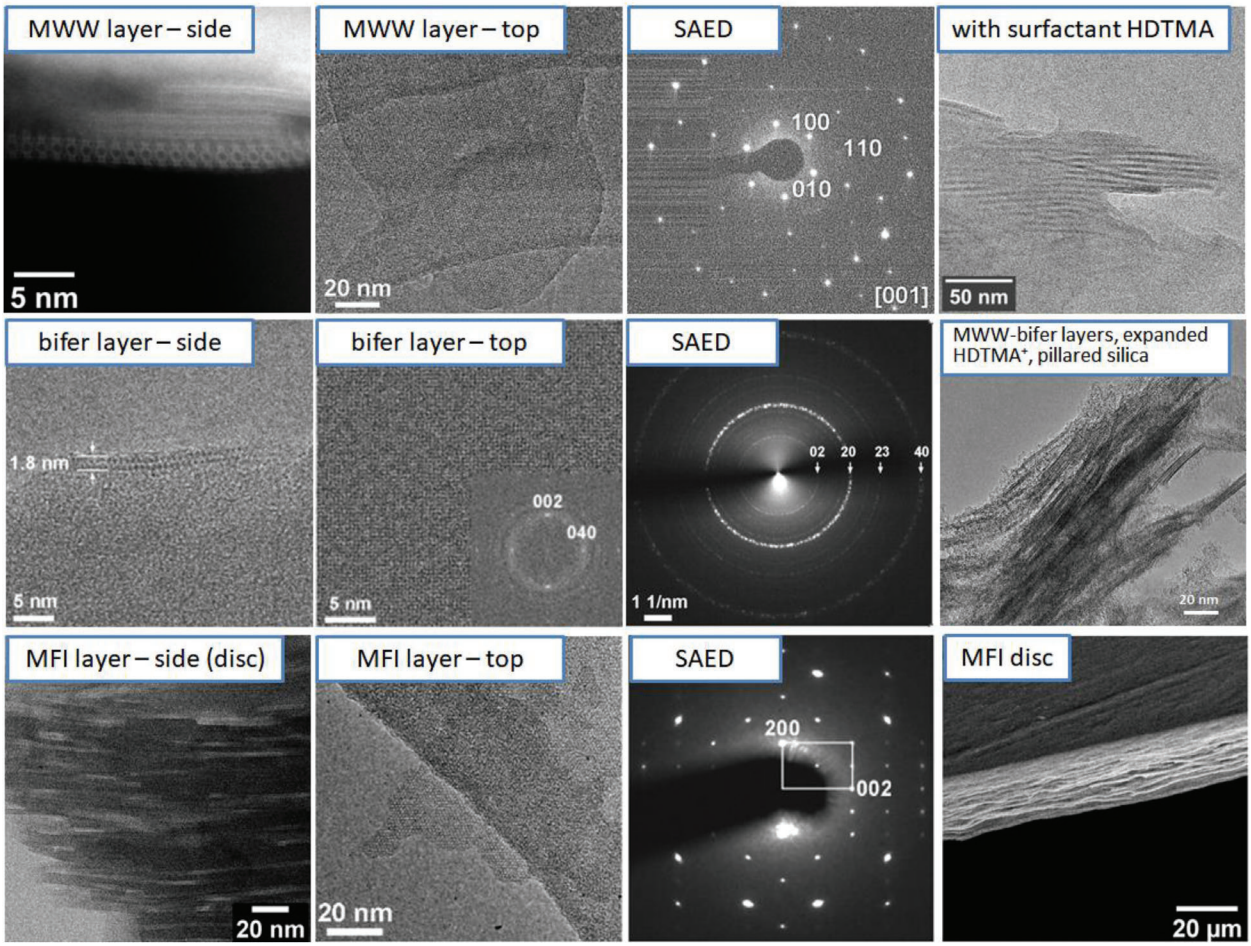

Figure 8. Electron microscopy images and SAED of MWW, bifer and MFI layers, MWW-surfactant composites (top right), pillared mixture of MWW and bifer layers (right center) and oriented MFI discs (right bottom). Reproduced under terms of the CC-BY license.[54] Copyright 2023, The Authors, published by The Royal Society of Chemistry.

described above. Once a system has been validated by these techniques, subsequent preparations can be verified by the reaction with HDTMA.

5. Preparation of Dispersed Nanosheets in Solution by Soft-Chemical Exfoliation

Layered zeolites can produce solutions of isolated free nanosheets directly in one step by contacting with moderately concentrated solutions, typically a few weight percent, of dispersing agents like tetrabutylammonium hydroxide, TBAOH. This reagent was effective with three zeolites: MWW, MFI, and bifer. Nanosheet solutions with lower concentration of the hydroxide may be preferred, e.g., in subsequent reactions with other reactants, in which case a two-step method is conveniently applied. The first step involves treatment with a more concentrated TBAOH solution, typically 10%, with stirring for 1–2 h. Centrifugation at 10 000 rpm for 20–60 min results in sedimentation of all solids. The obtained clear supernatant is decanted and discarded as it contains little or no dispersed nanosheets. This was ascertained by the addition of HDTMA cations, which did not produce solid as a proof of dispersed layers (see Section 4). The remaining solid is stirred with excess of water, 30–60 w/w, affording solutions of nanosheets with yields up to 70% or more, depending on a zeolite. The concentration of nanosheets is 1–2% and the typical pH is around 12 but can be lowered by dialysis or careful acidification. Solutions approaching neutral pH, e.g., by being subjected to dialysis, are not stable and result in slow flocculation. Sonication has been used to promote layer disorder in the synthesis of delaminated zeolites but its effect in the process of exfoliation of zeolites has not been systematically studied yet.[38,61]

The exfoliation of ilerite (RWR) was different and used a meglumine solution with pH = 9 with no agitation. In this case, TBAOH and other media proved ineffective.[53] The qualitative difference observed with ilerite was preservation of the original layer size, which is valuable and may be the ultimate goal in some applications. The authors emphasized spontaneous occurrence of the exfoliation of the layers without additional stimuli, like agitation or temperature. These are preconditions for preserving the pristine condition of layers and minimization of fragmentation. Another difference in comparison to the three zeolites treated with TBAOH is complete exfoliation of the entire sample, apparently without solid residue. This is a sample-dependent behavior,

quite rare since the presence of particles that remain unexfoliated is typical with the majority of layered materials. The most obvious explanation for the presence of nonexfoliating particles is presumed intergrowth but there may be other factors preventing liquid dispersion of the entire sample. Elimination of these adverse effects that reduce yield and quality may be important but for now is hard to approach in a systematic way.

The driving force for the exfoliation of 2D solids during the above treatments is recognized as (repulsive) osmotic swelling and has been recently proposed to be called 1D dissolution as a distinguishing phenomenon.[55] Ideally, it is expected to operate alone without additional stimuli but in practice additional actions like agitation through stirring for acceleration of the kinetics and diffusion as well as other enhancers can be useful. Detailed studies of the various effects during exfoliation are needed for better understanding and improvements. The first obvious factor to examine is the type/size of the cation, e.g., using smaller tetraalkylammonium cations (TPA, TEA, TMA).[116]

The critical characteristic of nanosheets is the charge, which for zeolite layers is not fixed, in contrast to other layers like clays and metal oxides,[62] although they may also exhibit variable charge in some cases.[117] Zeolites are carriers of a fixed charge related to acid sites generated by Al in the framework. This fixed charge is located mostly inside the layers and is compensated by templates from the original synthesis, so it is postulated to play a limited role in intercalation, delamination, and exfoliation of zeolite. If its role was decisive then expansion of zeolites should be possible by ion exchange at ambient pH, but it usually requires high pH, e.g., 12 or more. The basic environment produces deprotonation of silanol groups on the surface and possibly breaking of Si–O–Si bonds in the framework. The silanols are weakly acidic so their population and hence the layer charge will decrease with pH (OH^- concentration) in the surroundings. Lowering of this charge may result in layer association and other destabilizing phenomena, which presents another topic for inquiry. The density of silanols is determined primarily by the zeolite structure leading to expected differences for various frameworks. Notwithstanding the postulated limited contribution of zeolitic acid sites to the charge during exfoliation this aspect will have to be verified as well.

6. Methods of Isolating Exfoliated Layers and Their Characterization as Solids with Zeolite Properties

Exfoliated zeolite layers can be viewed as single crystals with high width-to-height (aspect) ratio and having the same structure as their 3D counterparts except for the terminal T-OH moieties on the surface. Their ability to produce active catalysts depends on demonstrating that treatments and exfoliation into monolayers and subsequent purification do not degrade the intrinsic zeolite acidity. It was shown before for a series of zeolite topologies, namely MWW, PCR, and MFI, by theoretical calculations with support of the experimental data that transition from 3D to 2D forms (formation of layered forms, not necessarily exfoliation) does affect zeolite acidity,[118] slightly lowering not only concentration but also strength of the Brønsted acid sites. On the other hand, Sauer reported, based on calculations for the CHA and FAU frameworks, that relative acid strength in zeolites is governed not only by the deprotonation energies (much lower for 2D zeolites) but also by interaction energies between the adsorbed/protonated molecule and the surface site. These effects were found to practically cancel out.[119] It is therefore essential for the appropriate assessment of acidity to use more than one technique to characterize exfoliated and subsequently recovered layers.

The earlier studies, focused on the preparation of membranes from exfoliated layers coated with surfactants, did not report the recovery of the nanosheets for the purpose of evaluating acidity or catalytic activity. It is often implied in the literature that reassembly of zeolite layers could produce hierarchical structure, for example, with edge-to-face elements, in which intercrystalline void spaces are connected with intralayer micropores. This should facilitate the transport of reagents and reduce diffusion constraints. An alternative possibility is that a face-to-face reassembly should be preferred, due to high aspect ratio, resulting in, at best, a modest porosity enhancement. To test these possibilities and the properties like acidity, the nanosheets in solution have been recovered and converted into the protonic form. This included purification steps such as removal of the residual template and cations (sodium) used in the synthesis, the agents used for exfoliation, and any other contaminants.

In general, colloids and larger particles in solution (including zeolite monolayers) can be flocculated by chemical coagulation, especially by addition of electrolytes or other reagents causing precipitation. These agents neutralize the charge of the dispersed particles destabilizing them and aiding aggregation, which leads to sedimentation. According to the IUPAC definition, flocculation (coagulation, agglomeration) is a process of contact and adhesion whereby dispersed particles are held together, leading to phase separation by the formation of precipitates of larger than colloidal size.[120]

The isolation of exfoliated MWW nanosheets[121] was induced by addition of alcohol or ammonium nitrate and by freeze-drying. The addition of electrolytes causes "salting out" due to increasing ionic strength.[122] The flocculation with ammonium nitrate was also testing the option of replacing sodium in lieu of ion exchange to generate acidic layers upon calcination. This attempt to eliminate the ion exchange step failed, resulting in products with inferior properties in comparison to the starting material and showing zero acidity. The flocculation with alcohol gave similar products. The 3rd tested method of isolation, freeze-drying, known as lyophilization, uses frozen solvent acting as a porogen that can create secondary pore system from the voids left upon removal of the solvent.[123] Freeze-drying of the solution with exfoliated nanosheets seemed to have positive influence on the structure of the recovered material, which became delicate and fluffy, requiring only slight crushing to obtain homogeneous powder.[124]

Dialysis was tested as an alternative to ion exchange as the required pretreatment of zeolite catalysts, for purification and removal of sodium cations from the solutions with MWW layers. After calcination and burning out of the organics, highly porous and acidic zeolite materials were obtained. The arrangement of layers in the resulting solid was not affected by dialysis, indicated by similar BET and external surface area values, which were comparable to those of the other flocculated solids obtained by different methods.[121]

Original methods of recovering exfoliated layers from the solutions were proposed by Breu et al.,[125,126] and included spray

Table 2. Representative acidic and textural properties for the starting zeolites and solid products obtained from the exfoliated dispersions by flocculation.

Sample	BAS[a] [μmol g^{-1}]	LAS[a] [μmol g^{-1}]	S_{BET}[b] [m^2 g^{-1}]	S_{ext}[c] [m^2 g^{-1}]	V_{micro}[d] [cm^3 g^{-1}]	Ref.
MCM-56 a	1155	99	457	180	0.09	
Layers from a	649	259	502	220	0.07	
MCM-56 b	778	97	467	167	0.09	
Layers from b	557	244	633	309	0.10	[51]
MCM-56 before dialysis	669	148	514	225	0.087	
Layers dialyzed and freeze-dried	598	180	566	171	0.108	[121]
MFI original layered	550	147	411	n/a	0.105	
MFI disc	571	110	447	n/a	0.130	[54]
Bifer layers	450	n/a	n/a	n/a	n/a	[52]

[a] Brønsted and Lewis acid sites; [b] total BET area; [c] external surface area; [d] micropore volume from t-plot.

coating, doctor blading, or slot die coating. These methods allow preparation of thin films, and orienting the nanosheets parallel to the substrate, exemplified by the prepared ilerite films, which proved to be excellent gas barriers.[53]

Zeolite nanosheets recovered from solutions have to be tested for quality and the preservation of zeolitic properties, especially when they are intended for use in catalysis. Since the resulting product is a solid, the structure may be evaluated by powder XRD, or infrared spectroscopy in the pseudoskeletal region, both by ATR and transmittance FT-IR after dilution in KBr.[121,127] The critical qualities are porosity and acidity, which may be evaluated by the standard methods of low temperature gas adsorption and desorption, and sorption of basic probe molecules followed by FT-IR spectroscopy, respectively.

X-ray diffraction patterns (XRDs) of the flocculated solids indicated preservation of the original zeolite structure and revealed spatial disorder with possible layer deformation upon reassembly suggested by lower scattering intensity.

The FT-IR spectroscopy data indicated preservation of the short-range order. The maxima characteristic of SBU units are present in the IR spectra of the crystalline zeolites. In some cases, as shown for MWW zeolites, the content of the crystalline phase can be qualitatively evaluated and even correlated with acidity.[127]

A summary of representative results, acid site concentration and BET surface areas, is presented in **Table 2**. In general, the recovered nanosheets showed some loss of acid site concentration but not by much, indicating high potential for acid catalysis. The concentration of Lewis acid sites increased by up to 2.5 times from the low level near 100 μmol g^{-1}. BET areas show moderate increases. Overall, the positive outcome is preservation of the basic zeolite qualities upon conversion into exfoliated layers and solid recovery. This is confirmed later upon catalytic testing discussed in Section 7.

7. Preparation of Intimate Mixtures of Different Zeolites and Composites with Nanoparticles and Clusters

One of the most notable benefits of exfoliated zeolite nanosheets in solution in comparison to the standard 3D crystals lies in the possibility of using the former to produce molecularly or sub-nanometer intimate composites with other active components including other zeolites, layered materials, nanoparticles, clusters and basically any compound or substance in a suitable form that can interact with the nanosheets.[54,128] Examples of unique materials are illustrated in **Figure 9**. It should be expected that there can be limitations to obtaining useful or desirable products due to thermodynamics and compatibility reasons like solubility and separation of phases, etc. An illustrative example is the reported mixing of two nanosheets resulting in a phase separation driven by so-called depletion effects.[129,130] A contrasting example shows that exfoliated zeolite nanosheets of different topologies can be mixed and retain homogeneous nature. They can be recovered as mixtures of layers and show activity better than sum of the parts.[52] Notwithstanding possible physical and chemical limitations, the solutions with zeolite nanosheets provide, in comparison to their solid analogues, enormously enriched latitude in designing nanoscale hybrids and composites. Furthermore, it should be expected that if simple combination of desired components is not effective, scientists will find ways to circumvent the obstacles. The benefits of bringing together components of various functionalities are illustrated by the particles of fluid cracking catalysts, which combine intimately several components with specific activity and roles to play.[131,132] The idea of combining different zeolites so that each can influence different molecules in the mixture has been also contemplated but could not be implemented at a sub-nanometer level due to the lack of suitable building blocks. Zeolite nanosheets fill this gap and proof-of-principle examples have been reported including intimate mixtures of MWW and MFI zeolites,[133] and MWW and bifer layers.[52] Mixtures of MWW zeolite nanosheets and MFI crystals were prepared by cocrystallization, i.e., synthesis of MFI in the presence of MWW monolayers, and by combination of MWW monolayers with already synthesized MFI crystals.[133] Zeolite MFI was deliberately chosen to be siliceous, i.e., catalytically inert, so that only the activity originating from the layers could be evaluated. Basic properties of the mixtures determined by FT-IR and nitrogen sorption were consistent with proportionate contribution from each (active and inactive) component. Catalytic evaluation suggested enhancement of activity indicated by the conversion not diminishing with decreasing content of the active MWW phase. Detailed discussion is continued in Section 8 focused on catalysis.

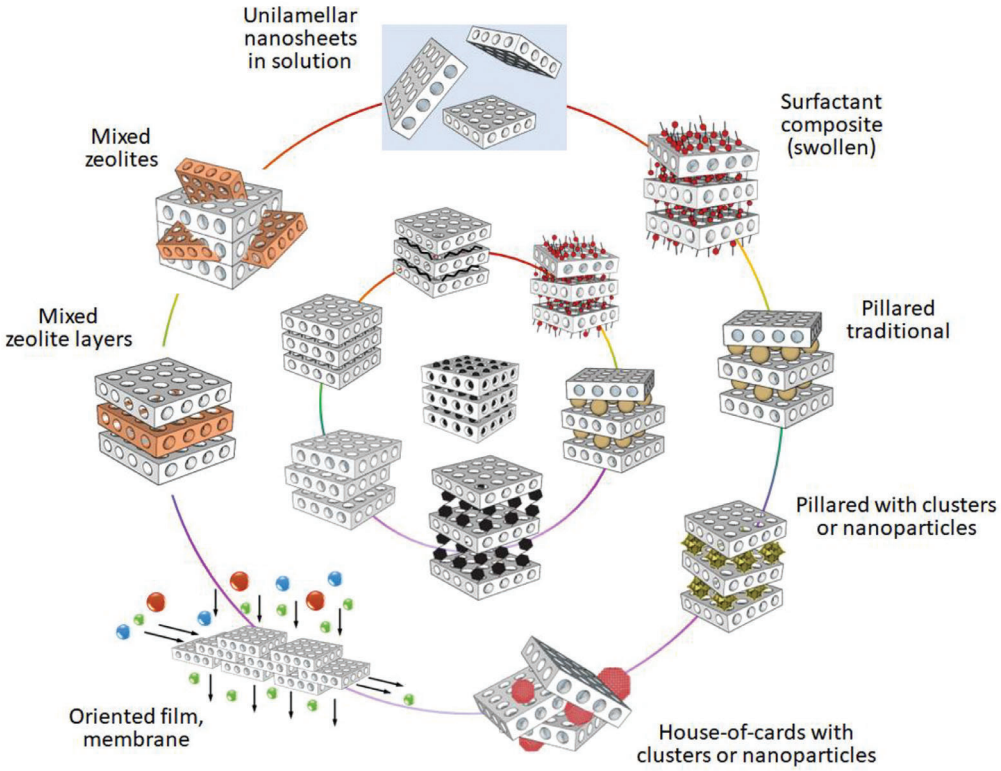

Figure 9. Increasing diversity of possible products that can be obtained upon progression from 3D frameworks (in the center), through 2D solids (2nd ring) to exfoliated monolayers in solution (3rd ring).

A variation on the same theme is making mixtures of nanosheets of different zeolites. This is limited for now because only MWW and bifer nanosheets are readily available in sufficient amounts.[52] The composite was obtained by mixing solutions of these layers, which did not produce precipitation. Addition of the surfactant HDTMA-Cl resulted in formation of a white solid with expanded basal spacing consistent with surfactant swollen nanosheet assemblies. The treatment with TEOS afforded pillared layered zeolite containing both MWW and bifer layers. Catalytic testing showed conversion in the mesitylene benzylation greater than sum of contribution from each component (based on % content).[52]

The last combination of active phases reported so far are MWW layers with Pt nanoparticles.[134] Related previous studies of these systems involved reacting MCM-22P precursor with MWW layers with the surfactant HDTMA and platinum precursor in DMF resulting in metal particles below 5 nm that were not sintering.[135] The preparation with nanosheets in solution involved adding solutions of Pt nanoparticles up to 1% wt/wt Pt to zeolite and isolation of solids by freeze-drying. Calcination caused some sintering to average ≈10 nm but there was no additional metal particle size increase afterward, even with repeated high temperature regeneration. Catalytic testing is elaborated in Section 8. Silanol groups on the surface of zeolite nanosheets are able to stabilize metal clusters and prevent their sintering even at high temperatures as evidenced for Rh clusters on IPC-1P layers.[136]

8. Catalytic Activity Alone and in Mixtures

Catalytic activity and industrial applications are the dominant areas of interest with zeolites hence new advances are examined instantly from the standpoint of potential benefits for catalysis.[131,137]

As a result of this interest, catalytic activity of exfoliated nanosheets was evaluated for the zeolite MWW after isolation from solution and activation by ion exchange and calcination.[51,52,121] The test reaction was alkylation of mesitylene with benzyl alcohol as one of the model systems for evaluating conversion of bulky reactants, which reflects acid site accessibility.[138] It has been often used to assess catalytic activity of hierarchical and layered zeolites.[139–142] Its purpose is to distinguish between transformations proceeding exclusively on the surface of zeolite catalyst (C-alkylation of mesitylene, targeted reaction) and in the pores (O-alkylation of benzyl alcohol, side reaction) as shown in **Figure 10**. In the C-alkylation, mesitylene is the largest reacting molecule, too big to enter micropores, and therefore produces bulky 2-benzyl-1,3,5-trimethylbenzene. The O-alkylation requires participation of relatively small benzyl alcohol molecules giving dibenzyl ether, which can be formed on both the external and internal acid sites. It is a reversible reaction and dibenzyl ether can be consumed providing the product for C-alkylation under appropriate conditions.[143]

Typical tests were carried out[51] with 50 mg of the hydrogen form of a zeolite, 0.1 g of dodecane as the internal

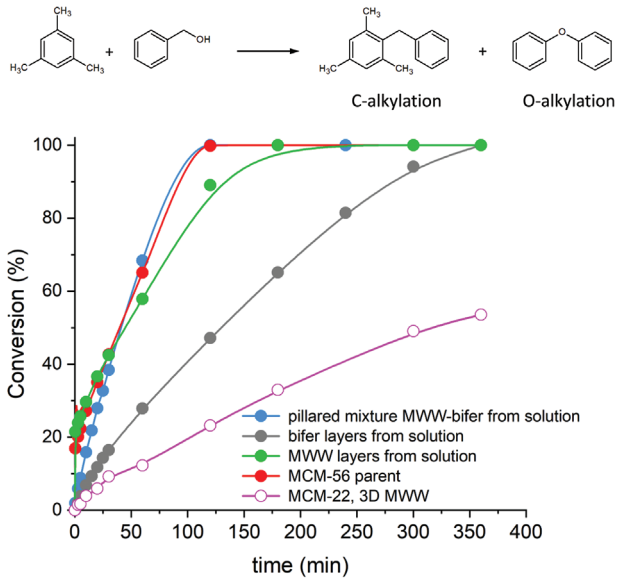

Figure 10. Catalytic activity, conversion versus time, of the exfoliated layered zeolites MWW, bifer and their pillared mixture, after recovery as solids compared to the parent sample MCM-56 and the 3D form of MWW (MCM-22).

chromatographic standard, and 22 ml of mesitylene, acting as both reagent and solvent, introduced into a 50 ml round-bottom flask. Stirring at >100 rpm was applied. After heating to the reaction temperature, 80°C, an aliquot of 0.2 g of benzyl alcohol (limiting reagent) was added with a syringe. Samples (250 µl) were withdrawn after 0.5, 3, 5, 10, 20, 30, 60, 120, 180, 300, and 360 min of the reaction time.

Catalytic activity of exfoliated MWW layers was evaluated after recovery from the solution, ion exchange and calcination. The conversion of benzyl alcohol in the model reaction was similar to the conversion exhibited by the parent MCM-56, as shown in Figure 10.[121] The latter is composed of disorganized MWW layers, so it is de facto a delaminated MWW with high Al content prepared by direct synthesis. For completeness, the corresponding 3D form of the MWW zeolite was obtained by calcination of the multilayered precursor MCM-22P and also tested catalytically. It showed much lower conversion as seen in Figure 10. The catalysts from exfoliated layers had enhanced textural characteristics in comparison to the parent, MCM-56, but it did not translate into higher activity.[121] These results show a very important point, that nanosheets exfoliated into solution and recovered can maintain high activity despite accompanying harsh treatments that can cause degradation of quality. The second conclusion is that disorganization of the layers, which is embodied by exfoliation and reassembly, does not by itself result in enhanced activity of a layered zeolite above that of the parent. To improve the performance, additional elements like incorporation of other components or different processing may be essential.

An example illustrating such activity uplift is the pillared MWW material obtained from exfoliated nanosheets. It was flocculated with the surfactant cation HDTMA (hexadecyltrimethylammonium) and pillared with TEOS (tetraethylorthosilicate).[144] The activity, conversion versus time (not presented in this paper), in the test mesitylene benzylation reaction was greater than that of the initial nonexfoliated zeolite MCM-56.[144] The conditions of pillaring, in particular high pH during flocculation and avoiding excess of the pillaring agent, were crucial for such enhanced activity and suggest further detailed studies.

Section 7 alluded to the fact that mixed zeolite catalysts containing 50% of zeolite layers as a sole active component may show the same activity as pure layers (100%). This was observed with the mixtures prepared from MWW layers and siliceous MFI. They were tested in the reaction of mesitylene with benzyl alcohol. The conversion with catalysts containing 50% of inert MFI was the same as with pure MWW layers, so was apparently not diminished by dilution of the active component to one half. Further reduction of the content of MWW did cause reduction of the conversion rate. A physical mixture of the starting MWW parent and MFI crystals was also less active. This retention of activity upon dilution of active zeolite layers can be exploited to include in the mixture another active component with additional or complementing functionality. The outcome may be synergistic enhancement of activity or creation of a new type of activity in terms of kinetics and products. A similar situation was observed with the mixture of layers – MWW and bifer as described above. It was obtained by mixing solutions of both types of nanosheets, flocculation with surfactant and pillaring with TEOS. Subsequent catalytic testing showed conversion in the mesitylene benzylation that was higher than the sum of contributions from each component (based on % content). This reveals the potential of such mixed systems for activity enhancement or modification.

Another example of composites obtained from exfoliated zeolites is illustrated by the platinum activated MWW layers with up to 1% of Pt nanoparticles.[134] The catalysts were obtained by mixing solutions of nanosheets and Pt nanoparticles and isolation by freeze-drying. The test reaction was hydrogenation of 3-nitrotoluene. The observed activity was comparable to a commercial sample of 1% Pt deposited on alumina obtained from a vendor. The top activity was reached already at 0.3% Pt and levelled off with increasing Pt content.

The results of catalytic activity with the illustrated mixed systems underscore the potential for exploiting exfoliated nanosheets in combinations with other components. The possibilities are practically unlimited, unlike with 3D zeolites and even 2D solids, allowing intimate combination with any ingredients, layers, nanoparticles, etc. There is little precedence with designing such systems because this option was unavailable until exfoliated zeolite layers emerged. Attractive combinations seem to be mixing medium pore layers like MWW with larger pore zeolites (FAU, beta) or mesoporous materials, active nanoparticles like ceria or titania. They can be readily combined with exfoliated layers and afford dual reactivity.

9. Preparation of Oriented Films and Membranes with Exfoliated Zeolite

Exfoliation provides zeolites in a novel form, different from the standard polycrystalline powders that are generally used as-made without substantial alteration of the macrostructure. The availability of nanosheets in solution allows the design of new materials and applications that have been impossible or unimaginable

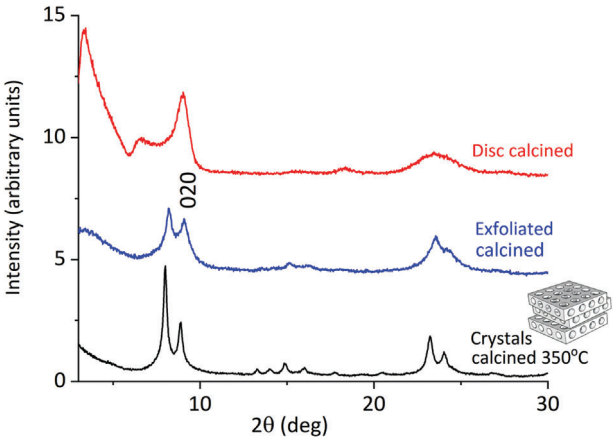

Figure 11. XRD identification of oriented MFI films based on comparison with powder and disorganized layers. The 020 label refers to the peak of the 3D MFI, which is also exhibited in the disc pattern and confirms planar orientation of the layers.

with the conventional zeolite crystals. There are not many concrete ideas for that, mainly because the lack of suitable precursors has not encouraged contemplation of how they could be used to exploit the unique zeolite properties: active and porous layers. Zeolite layers in solution present the problem of availability in large quantities and sufficient concentrations, which makes them less competitive for traditional catalytic applications, which require high volumes. However, they may be suitable for low volume high value applications exemplified by membranes.[145] Earlier studies with dispersed zeolite layers obtained via the surfactant pre-expansion route, showed their usefulness for preparation of oriented membranes. The obtained membranes contained defects, especially after calcination, but they could be cured, and were tested for gas separations. The membranes prepared with zeolites MFI, MWW, and SOD showed promising performances.[44,45]

The primary advantage of the present nanosheets obtained by direct exfoliation is availability and easy preparation – a solid sample can be converted in a few hours in 2 easy steps into a solution with exfoliated layers that can be immediately used for the preparation of films. Simple filtration was shown to afford films and transparent self-standing discs that can be ion exchanged and calcined to activate pores and acid sites.[51,54] XRD patterns confirmed strict orientation expected for high aspect ratio particles by showing only purely interplanar reflection with two Miller indices equal to 0. As-synthesized and calcined films showed different basal spacings. The former was greater than the crystallographic unit cell of the corresponding 3D framework. This apparent expansion is readily rationalized by surface termination with silanols and additional molecules intercalated between layers – water and to a smaller extent organics. Films made of MFI layers presented an intriguing and more complex situation, which is attributed to the fact that the layer thickness was 1.5 times of the unit cell—3.0 nm versus 2.0 nm for the corresponding *b* unit axis. As a results 2 sets of 0k0 reflections can be observed in the XRD, see **Figure 11**. Those based on the unit cell include a prominent 020 peak at 9° 2θ. A typical zeolite MFI XRD pattern shows a doublet with peaks at 8 and 9° 2θ but the former originates from reflections with nonzero h or l indices. These latter reflections are absent in the XRD of obtained films, which proves the b orientation. Standard MFI does not show low angle XRD peaks below the 8°–9° 2θ doublet. In contrast, the MFI films show additional reflections at lower 2θ angles that appear as orders of the basal spacing slightly greater than 3.0 nm and 6.0 nm for surfactant precipitated MFI layers. The latter indicates swollen-like MFI layers. Calcination results in contraction in both cases to ≈2.8 nm *d*-spacing indicated by two asymmetric peaks at 2.8 and 1.4 nm. This contraction below the nominal layer thickness is also characteristic for laterally disorganized zeolite layers, which can produce upon calcination materials called subzeolites.[146] Their formation can be explained by uneven surfaces of zeolite layers with high points and troughs. The high points (representing limits of the layer thickness) can end up in valleys reducing the apparent interlayer repeat. The studies on producing zeolite films and discs from directly exfoliated zeolite nanosheets in solution have not been extended beyond the preparation and characterization. Meaningful testing for applications such as gas sieving, possible catalysis by oriented zeolites, etc. require advanced dedicated equipment and preparation. They are simply beyond technical capabilities in a conventional laboratory setting but are expected to find interest in due time.

This potential of using exfoliated nanosheets to produce gas separation zeolite membrane is illustrated by a recent study reporting hydrogen purification membrane prepared from a layered zeolite denoted ECNU-28.[66] As-synthesized ECNU-28 material was first treated with an acid to remove the organic template and then dispersed in DMF. The suspension contained both mono- and multilayered nanosheets but produced a working membrane after filtration and defect repair. The structural characterization and identity of ECNU-28 raise serious doubts for several reasons. ECNU-28 and bifer have similar XRD patterns and unit cells, which suggests identical or similar structure. Minor differences in the XRD patterns can be attributed to typical variation of the XRDs of layered materials depending on the preparation and treatments. The questionable aspects include the proposed swollen structure of ECNU-28 with 0.81 nm thick inorganic layers, separated by 1.53 nm organic interlayer containing vertical decamethonium templates and the overall structure identification as the SZR zeolite. The proposed swollen structure is inconsistent with the determined relatively low organic content of 18% which should be much higher, closer to 50%, for a truly swollen precursor. All other data (XRD, TEM, AFM) suggest doubled layer thickness, comparable to bifer. The proposed SZR structure is based on qualitative comparison of calculated and experimental XRD and ED patterns, the latter obtained with a polycrystalline sample. Doubts about the structure assignment can be also raised based on the synthesis—the SZR framework is not easy to synthesize and so far has been obtained only with potassium in the gel,[147] which is not used in this case. The topology of bifer is unknown so it is important to continue investigation of the structure of ECNU-28 and its relation to bifer.

10. Perspectives Beyond Traditional Zeolite Applications

Zeolite nanosheets straddle two structurally and frequently chemically different classes of solids: 3D porous materials and

2D ultrathin layers. Summarizing the above data and discussion there are two basic takeaways pertinent to their practical potential. First, unmodified zeolite nanosheets are usually not much better catalytically than conventional 3D zeolites and in particular do not produce significantly more porous structures without additional help. Second, these nanosheets readily produce oriented films, which can be competitive in special applications that can tolerate increased cost of preparation. Regarding the first, zeolite nanosheets are unlikely replacement of catalysts in the conventional large-scale processes. However, as illustrated above and in Figure 9, they can be used to produce nanohybrid materials that their 3D counterparts cannot. This, in combination with the possibility of easy and reliable production of films can be useful not only for membrane fabrication as already demonstrated but also in catalysis on surfaces and by thin films. This method can supply new types of materials with well-defined surfaces that can differ for each zeolite topology. For starters, this can be a valuable research tool of reaction mechanisms because of precise knowledge of the surface that can be modified through surface charge, silanol density, heteroatoms, etc. Hence, investigation of model reactions can provide insights that may be obfuscated with polycrystalline samples, which do not allow much control over exposure of particular crystal faces. The potential learnings may allow tuning of surface properties and consequently reactivity. From the perspective of zeolite formation mechanism and stability, the films can be used as substrates for immobilization and investigation of guest molecules, e.g., various structure directing agents. Going further, as nanosheets allow unhindered combination with other entities like clusters, nanoparticles and other layers, the resulting hybrid precursors can be also deposited on supports and investigated. Needless to say, the nonzeolite components can have alternative activity, e.g., redox, photocatalytic, etc., and result in multifunctional catalysts. Nanoparticles of titania, ceria and other metal oxides have proven catalytic activity that can complement zeolites.

Looking from side of the 2D solids, zeolite nanosheets can be considered for the various applications unrelated to catalysis. The examples include protective covering (anticorrosion, flame retardant, etc.),[55] design of functional composite materials via LbL (layer by layer) deposition,[50] and bio-med applications like drug delivery.[148] In this regard, they are in competition with many established and already extensively studied other 2D solids, but have different structures and additional features already mentioned—pores and active sites.[32,75,149]

The applications of 2D solids often invoke special optical, electric, electronic and magnetic properties for exploitation in various situations and devices.[150] Zeolite nanosheets do not possess such special characteristics but may be used in combination with these materials for example as insulators or separators between physically active layers. The special trait of zeolite layers, namely internal porosity, may be exploited in a way that the the other 2D solids cannot offer. This could be exploited for introduction in the pores of selected ions or moieties capable of imparting specific properties: optical, magnetic, electronic, electric conductance as alternatives to other layers with these qualities. It may even be possible to vary the magnitude of particular effects by changing the amount of introduced species in the pores. The pores in the layers can also be used as "dynamic" gas barriers, so named because they can prevent not only diffusion through but also adsorb external molecules. Applications as sensing devices are also attractive for zeolite films.

In summary, zeolite nanosheets are promising objects to study for applications specific to zeolites and 2D solids with a particular focus on the exploitation as oriented films in catalysis and special devices. The trait that distinguishes zeolite nanosheets from other 2D solids, i.e., the presence of internal pores and exchangeable sites, may be a particular fulcrum toward valuable unique applications.

Since zeolite nanosheets in solution were not available until recently there has been very little attention or contemplation of their possible uses beyond generic, already mentioned applications as both zeolites and layered materials. The enabled capabilities for thin zeolite film fabrication have been unavailable hence there is little prior art or even conceptual planning for the design of viable schemes. Specific uses can only be speculative, especially because the mentioned classes of materials provide abundant prior art with proven usages and benefits. The pursuit of practical application requires expanding knowledge about preparation and properties of exfoliated zeolite nanosheets. The primary objectives are expanding the exfoliation to other frameworks and understanding synthesis parameters that influence formation of intergrowth and thus affect the amount of nanosheets that can exfoliate directly. There are many aspects of the exfoliation and the nanosheet properties that are little known, like distribution of lateral sizes, quality preservation, association upon standing and possibility for using different exfoliation agents and solvents. Each of these parameters may be important in specific instances so they deserve systematic examination.

Summarizing, readily available exfoliated zeolite nanosheets are novel, so there was no time to document applications and show their importance except by inference from other inorganic nanosheets. There is already evidence of their value for synthesizing oriented discs both porous[44,48] and impermeable[53] by choosing different frameworks. The importance of inorganic nanosheets is underscored by frequently published reviews on topics including uses in catalysis,[151] biomedical applications,[148,152] to make heterostructures[153] and functional devices.[154] As was emphasized, zeolite nanosheets exhibit new functionalities to exploit: strong catalytic activity and layer porosity. They can be instantly considered for catalysis and comparison with clays, e.g., in biomedical applications. Specific uses will depend on particular needs and testing, which are hard to predict. What is particularly promising about exfoliated zeolite nanosheets is easy preparation and genuine versatility for the preparation of nanoscale composites because of availability in the dispersed liquid state. This opens enormous opportunities in comparison to the reliance on solid systems as substrates for syntheses.

Acknowledgements

This work was financed with the funds from the National Science Centre Poland, grant no. 2020/37/B/ST5/01258 (W.J.R, B.G.). M.M. and J.C. thank the Czech Science Foundation for funding this research through the ExPro project (19–27551X) and OP VVV "Excellent Research Teams," project no. Z.02.1.01/0.0/0.0/15_003/0000417 – CUCAM from Ministerstvo Školství, Mládeže a Tělovýchovy. M.O. thanks Ministry of Education, Youth and Sports of Czech Republic for funding through ERC_CZ project LL 2104. T.S. acknowledges Japan Science and Technology Agency (JST),

Grant No. JPMJCR17N1 (CREST) and Japan Society for the Promotion of Science (JSPS), Grant No. P21036. The work was also supported by Ministerstvo Školství, Mládeže a Tělovýchovy as ERDF/ESF project TECHSCALE (Nos. CZ.02.01.01/00/22_008/0004587).

Conflict of Interest

The authors declare no conflict of interest.

Keywords

bifer, chemical exfoliation, ilerite, nanocomposites, ultrathin zeolite nanosheets, zeolite films, zeolites MFI and MWW

Received: July 24, 2023
Revised: September 15, 2023
Published online: November 28, 2023

[1] P. Van Der Voort, K. Leus, E. De Canck, *Introduction to Porous Materials*, Wiley, New York, NY, USA, **2019**.
[2] J. Rouquerol, F. Rouquerol, P. Llewellyn, G. Maurin, K. S. W. Sing, *Adsorption by Powders and Porous Solids: Principles, Methodology and Applications*, Elsevier Science, Amsterdam **2013**.
[3] F. Schüth, K. S. W. Sing, J. Weitkamp, *Handbook of Porous Solids*, Wiley, New York, NY **2002**.
[4] D. W. Breck, *Zeolite Molecular Sieves: Structure, Chemistry, and Use*, Wiley, New York, NY **1973**.
[5] R. M. Milton, *ACS Symp. Ser.* **1989**, *398*, 1.
[6] R. M. Barrer, *Pure Appl. Chem.* **1986**, *58*, 1317.
[7] S. M. Csicsery, *Pure Appl. Chem.* **1986**, *58*, 841.
[8] I. Fechete, J. Vedrine, *Molecules* **2015**, *20*, 5638.
[9] T. F. Degnan, Jr., *Stud. Surf. Sci. Catal.* **2007**, *170*, 54.
[10] D. E. W. Vaughan, *Catal. Today* **1988**, *2*, 187.
[11] C. T. Kresge, M. E. Leonowicz, W. J. Roth, J. C. Vartuli, J. S. Beck, *Nature* **1992**, *359*, 710.
[12] J. S. Beck, J. C. Vartuli, W. J. Roth, M. E. Leonowicz, C. T. Kresge, K. D. Schmitt, C. T. W. Chu, D. H. Olson, E. W. Sheppard, S. B. Mccullen, J. B. Higgins, J. L. Schlenker, *J. Am. Chem. Soc.* **1992**, *114*, 10834.
[13] U. Ciesla, F. Schüth, *Microporous Mesoporous Mater.* **1999**, *27*, 131.
[14] O. M. Yaghi, M. O'Keeffe, N. W. Ockwig, H. K. Chae, M. Eddaoudi, J. Kim, *Nature* **2003**, *423*, 705.
[15] A. Khobotov-Bakishev, L. Hernández-López, C. Von Baeckmann, J. Albalad, A. Carné-Sánchez, D. Maspoch, *Adv. Sci.* **2022**, *9*, 2104753.
[16] J. V. Smith, *Chem. Rev.* **1988**, *88*, 149.
[17] S. L. Suib, J. Prech, E. Szaniawska, J. Čejka, *Chem. Rev.* **2023**, *123*, 877.
[18] R. M. Barrer, *Hydrothermal Chemistry of Zeolites*, Academic, San Diego, CA, **1982**.
[19] J. Čejka, A. Corma, S. I. Zones, *Zeolites and Catalysis: Synthesis, Reactions and Applications*, Wiley, New York, NY **2010**.
[20] M. E. Davis, *Ind. Eng. Chem. Res.* **1991**, *30*, 1675.
[21] C. Baerlocher, L. B. McCusker, D. H. Olson, *Atlas of Zeolite Framework Types*, Elsevier, Amsterdam, **2007**.
[22] S. I. Zones, *Micropor. Mesopor. Mater.* **2011**, *144*, 1.
[23] M. K. Rubin, P. Chu, *Composition of Synthetic Porous Crystalline Material, Its Synthesis and Use, U.S. Patent, Mobil Oil Corp. US*, **1990**.
[24] T. F. Degnan, C. M. Smith, C. R. Venkat, *Appl. Catal., A* **2001**, *221*, 283.
[25] I. Fechete, Y. Wang, J. C. Védrine, *Catal. Today* **2012**, *189*, 2.
[26] M. E. Leonowicz, J. A. Lawton, S. L. Lawton, M. K. Rubin, *Science* **1994**, *264*, 1910.
[27] S. L. Lawton, A. S. Fung, G. J. Kennedy, L. B. Alemany, C. D. Chang, G. H. Hatzikos, D. N. Lissy, M. K. Rubin, H.-K. C. Timken, S. Steuernagel, D. E. Woessner, *J. Phys. Chem.* **1996**, *100*, 3788.
[28] L. Schreyeck, P. Caullet, J.-C. Mougenel, J.-L. Guth, B. Marler, *J. Chem. Soc., Chem. Commun.* **1995**, 2187.
[29] W. J. Roth, P. Nachtigall, R. E. Morris, J. Čejka, *Chem. Rev.* **2014**, *114*, 4807.
[30] B. Marler, H. Gies, *Eur. J. Mineral.* **2012**, *24*, 405.
[31] S. M. Auerbach, K. A. Carrado, P. K. Dutta, *Handbook of Layered Materials*, Marcel Dekker, New York, NY **2004**.
[32] V. Nicolosi, M. Chhowalla, M. G. Kanatzidis, M. S. Strano, J. N. Coleman, *Science* **2013**, *340*, 1226419.
[33] W. J. Roth, C. T. Kresge, J. C. Vartuli, M. E. Leonowicz, A. S. Fung, S. B. McCullen, *Stud. Surf. Sci. Catal.* **1995**, *94*, 301.
[34] M. E. Landis, B. A. Aufdembrink, P. Chu, I. D. Johnson, G. W. Kirker, M. K. Rubin, *J. Am. Chem. Soc.* **1991**, *113*, 3189.
[35] M. Hartmann, *Angew. Chem., Int. Ed.* **2004**, *43*, 5880.
[36] R. Millini, G. Perego, W. O. Parker Jr, G. Bellussi, L. Carluccio, *Microporous Mater.* **1995**, *4*, 221.
[37] M. Opanasenko, W. O. Parker, M. Shamzhy, E. Montanari, M. Bellettato, M. Mazur, R. Millini, J. Čejka, *J. Am. Chem. Soc.* **2014**, *136*, 2511.
[38] A. Corma, V. Fornes, S. B. Pergher, T. L. M. Maesen, J. G. Buglass, *Nature* **1998**, *396*, 353.
[39] W. J. Roth, P. Nachtigall, R. E. Morris, P. S. Wheatley, V. R. Seymour, S. E. Ashbrook, P. Chlubná, L. S. Grajciar, M. Polozij, A. Zukal, O. Shvets, J. Čejka, *Nat. Chem.* **2013**, *5*, 628.
[40] P. Eliášová, M. Opanasenko, P. S. Wheatley, M. Shamzhy, M. Mazur, P. Nachtigall, W. J. Roth, R. E. Morris, J. Čejka, *Chem. Soc. Rev.* **2015**, *44*, 7177.
[41] W. J. Roth, B. Gil, W. Makowski, A. Slawek, J. Grzybek, M. Kubu, J. Cejka, *Chem. Mater.* **2016**, *28*, 3616.
[42] E. Schulman, W. Wu, D. X. Liu, *Materials* **2020**, *13*, 1822.
[43] T. Nakato, J. Kawamata, S. Takagi, *Inorganic Nanosheets and Nanosheet-Based Materials: Fundamentals and Applications of Two-Dimensional Systems*, Springer, Japan **2017**.
[44] K. Varoon, X. Zhang, B. Elyassi, D. D. Brewer, M. Gettel, S. Kumar, J. A. Lee, S. Maheshwari, A. Mittal, C.-Y. Sung, M. Cococcioni, L. F. Francis, A. V. McCormick, K. A. Mkhoyan, M. Tsapatsis, *Science* **2011**, *334*, 72.
[45] M. Dakhchoune, L. F. Villalobos, R. Semino, L. Liu, M. Rezaei, P. Schouwink, C. E. Avalos, P. Baade, V. Wood, Y. Han, M. Ceriotti, K. V. Agrawal, *Nat. Mater.* **2021**, *20*, 362.
[46] S. Sabnis, V. A. Tanna, C. Li, J. Zhu, V. Vattipalli, S. S. Nonnenmann, G. Sheng, Z. Lai, H. H. Winter, W. Fan, W. Fan, *Chem. Commun.* **2017**, *53*, 7011.
[47] N. Rangnekar, M. Shete, K. V. Agrawal, B. Topuz, P. Kumar, Q. Guo, I. Ismail, A. Alyoubi, S. Basahel, K. Narasimharao, C. W. Macosko, K. A. Mkhoyan, S. Al-Thabaiti, B. Stottrup, M. Tsapatsis, *Angew. Chem., Int. Ed.* **2015**, *54*, 6571.
[48] K. V. Agrawal, *Chimia* **2018**, *72*, 313.
[49] T. Maluangnont, Y. Yamauchi, T. Sasaki, W. J. Roth, J. Cejka, M. Kubu, *Chem. Commun.* **2014**, *50*, 7378.
[50] T. Taniguchi, L. Nurdiwijayanto, R. Ma, T. Sasaki, *Appl. Phys. Rev.* **2022**, *9*, 021313.
[51] W. J. Roth, T. Sasaki, K. Wolski, Y. Song, D.-M. Tang, Y. Ebina, R. Ma, J. Grzybek, K. Kalahurska, B. Gil, M. Mazur, S. Zapotoczny, J. Cejka, *Sci. Adv.* **2020**, *6*, eaay8163.
[52] W. J. Roth, T. Sasaki, K. Wolski, Y. Ebina, D.-M. Tang, Y. Michiue, N. Sakai, R. Ma, O. Cretu, J. Kikkawa, K. Kimoto, K. Kalahurska, B. Gil, M. Mazur, S. Zapotoczny, J. Cejka, J. Grzybek, A. Kowalczyk, *J. Am. Chem. Soc.* **2021**, *143*, 11052.
[53] P. Loch, D. Schuchardt, G. Algara-Siller, P. Markus, K. Ottermann, S. Rosenfeldt, T. Lunkenbein, W. Schwieger, G. Papastavrou, J. Breu, *Sci. Adv.* **2022**, *8*, eabn9084.

[54] W. J. Roth, T. Sasaki, K. Wolski, B. Gil, S. Zapotoczny, J. Cejka, M. Kubu, M. Mazur, Y. Ebina, N. Sakai, D.-M. Tang, R. Ma, *Inorg. Chem. Front.* **2023**, *10*, 1511.
[55] V. Dudko, O. Khoruzhenko, S. Weiß, M. Daab, P. Loch, W. Schwieger, J. Breu, *Adv. Mater. Technol.* **2023**, *8*, 2200553.
[56] *The Clay Minerals Society Glossary for Clay Science Project*, https://www.clays.org/clay_glossary/, (accessed: July 2023).
[57] M. V. Opanasenko, W. J. Roth, J. Cejka, *Catal. Sci. Technol.* **2016**, *6*, 2467.
[58] A. Okrut, M. Aigner, C. Schöttle, N. A. Grosso-Giordano, S.-J. Hwang, X. Ouyang, S. Zones, A. Katz, *Dalton Trans.* **2018**, *47*, 15082.
[59] Y. Zhou, Y. Mu, M.-F. Hsieh, B. Kabius, C. Pacheco, C. Bator, R. M. Rioux, J. D. Rimer, *J. Am. Chem. Soc.* **2020**, *142*, 8211.
[60] A. Corma, V. Fornés, J. Martinez-Triguero, S. B. Pergher, *J. Catal.* **1999**, *186*, 57.
[61] P. Frontera, F. Testa, R. Aiello, S. Candamano, J. B. Nagy, *Microporous Mesoporous Mater.* **2007**, *106*, 107.
[62] N. Miyamoto, Y. Ohsedo, T. Nakato, *Colloidal Nanosheets* (Eds: T. Nakato, J. Kawamata, S. Takagi) Inorganic Nanosheets and Nanosheet-Based Materials: Fundamentals and Applications of Two-Dimensional Systems, Springer, Berlin **2017**, pp. 201–260.
[63] X. Ouyang, S.-J. Hwang, R. C. Runnebaum, D. Xie, Y.-J. Wanglee, T. Rea, S. I. Zones, A. Katz, *J. Am. Chem. Soc.* **2014**, *136*, 1449.
[64] I. Ogino, E. A. Eilertsen, S.-J. Hwang, T. Rea, D. Xie, X. Ouyang, S. I. Zones, A. Katz, *Chem. Mater.* **2013**, *25*, 1502.
[65] W. J. Roth, *Stud. Surf. Sci. Catal.* **2005**, *158A and B*, 19.
[66] J. L. Wang, Y. Q. Fan, J. A. Jiang, Z. Wan, S. Y. Pang, Y. J. Guan, H. Xu, X. He, Y. H. Ma, A. S. Huang, P. Wu, *Angew. Chem., Int. Ed.* **2023**, *62*, 202304734.
[67] W. J. Roth, *Stud. Surf. Sci. Catal.* **2007**, *168*, 221.
[68] A. R. Urade, I. Lahiri, K. S. Suresh, *JOM* **2023**, *75*, 614.
[69] J. Du, G. Fu, X. Xu, A. M. Elshahawy, C. Guan, *Small* **2023**, *19*, 2207833.
[70] V. B. Mohan, K.-T. Lau, D. Hui, D. Bhattacharyya, *Composites, Part B* **2018**, *142*, 200.
[71] X. B. Liu, Z. K. Kou, S. C. Mu, *Prog. Chem.* **2015**, *27*, 1566.
[72] P. Tao, S. Yao, F. Liu, B. Wang, F. Huang, M. Wang, *J. Mater. Chem. A* **2019**, *7*, 23512.
[73] J. R. Prekodravac, D. P. Kepic, J. C. Colmenares, D. A. Giannakoudakis, S. P. Jovanovic, *J. Mater. Chem. C* **2021**, *9*, 6722.
[74] A. Gutiérrez-Cruz, A. R. Ruiz-Hernández, J. F. Vega-Clemente, D. G. Luna-Gazcón, J. Campos-Delgado, *J. Mater. Sci.* **2022**, *57*, 14543.
[75] W. J. Roth, B. Gil, W. Makowski, B. Marszalek, P. Eliasova, *Chem. Soc. Rev.* **2016**, *45*, 3400.
[76] M. Choi, K. Na, J. Kim, Y. Sakamoto, O. Terasaki, R. Ryoo, *Nature* **2009**, *461*, 246.
[77] H. Y. Luo, V. K. Michaelis, S. Hodges, R. G. Griffin, Y. Román-Leshkov, *Chem. Sci.* **2015**, *6*, 6320.
[78] M. Mazur, P. S. Wheatley, M. Navarro, W. J. Roth, M. Polozij, A. Mayoral, P. Eliasova, P. Nachtigall, J. Cejka, R. E. Morris, *Nat. Chem.* **2016**, *8*, 58.
[79] A. U. Rehman, D. Arepalli, S. F. Alam, M.-Z. Kim, J. Choi, C. H. Cho, *Nanomaterials* **2021**, *11*, 2327.
[80] K. V. Agrawal, B. Topuz, Z. Jiang, K. Nguenkam, B. Elyassi, L. F. Francis, M. Tsapatsis, M. Navarro, *Open Med. Chem. J.* **2013**, *59*, 3458.
[81] C. N. Zhang, S. N. Wang, H. B. Zhang, P. Liu, M. M. Yu, G. X. Zhong, H. H. Zhang, H. Y. Lu, S. Y. Xu, S. Dong, X. Y. Guan, Y. Tang, *Macromol. Mater. Eng.* **2020**, *305*, 2000406.
[82] S. Sabnis, V. A. Tanna, J. Gulbinski, J. Zhu, S. S. Nonnenmann, G. Sheng, Z. Lai, H. H. Winter, W. Fan, *Microporous Mesoporous Mater.* **2021**, *315*, 110883.
[83] H. Zhang, Q. Xiao, X. Guo, N. Li, P. Kumar, N. Rangnekar, M. Y. Jeon, S. Al-Thabaiti, K. Narasimharao, S. N. Basahel, B. Topuz, F. J. Onorato, C. W. Macosko, K. A. Mkhoyan, M. Tsapatsis, *Angew. Chem., Int. Ed.* **2016**, *55*, 7184.
[84] L. Niu, J. N. Coleman, H. Zhang, H. Shin, M. Chhowalla, Z. Zheng, *Small* **2016**, *12*, 272.
[85] C. Hermosa, B. R. Horrocks, J. I. Martínez, F. Liscio, J. Gómez-Herrero, F. Zamora, *Chem. Sci.* **2015**, *6*, 2553.
[86] D. N. Bunck, W. R. Dichtel, *J. Am. Chem. Soc.* **2013**, *135*, 14952.
[87] T. J. Mason, J. P. Lorimer, *Applied Sonochemistry: The Uses of Power Ultrasound in Chemistry and Processing*, Wiley-VCH, Darmstadt, Germany **2002**.
[88] S. Maheshwari, E. Jordan, S. Kumar, F. S. Bates, R. L. Penn, D. F. Shantz, M. Tsapatsis, *J. Am. Chem. Soc.* **2008**, *130*, 1507.
[89] I. Ogino, M. M. Nigra, S.-J. Hwang, J.-M. Ha, T. Rea, S. I. Zones, A. Katz, *J. Am. Chem. Soc.* **2011**, *133*, 3288.
[90] W. J. Roth, J. Cejka, R. Millini, E. Montanari, B. Gil, M. Kubu, *Chem. Mater.* **2015**, *27*, 4620.
[91] S. Maheshwari, C. Martínez, M. Teresa Portilla, F. J. Llopis, A. Corma, M. Tsapatsis, *J. Catal.* **2010**, *272*, 298.
[92] M. Y. Jeon, D. Kim, P. Kumar, P. S. Lee, N. Rangnekar, P. Bai, M. Shete, B. Elyassi, H. S. Lee, K. Narasimharao, S. N. Basahel, S. Al-Thabaiti, W. Xu, H. J. Cho, E. O. Fetisov, R. Thyagarajan, R. F. Dejaco, W. Fan, K. A. Mkhoyan, J. I. Siepmann, M. Tsapatsis, *Nature* **2017**, *543*, 690.
[93] D. Kim, S. Ghosh, N. Akter, A. Kraetz, X. Duan, G. Gwak, N. Rangnekar, J. R. Johnson, K. Narasimharao, M. A. Malik, S. Al-Thabaiti, B. Mccool, J. A. Boscoboinik, K. A. Mkhoyan, M. Tsapatsis, *Sci. Adv.* **2022**, *8*, eabm8162.
[94] C. Zhang, F. Lin, L. Kong, Z. Ye, D. Pan, H. Li, H. Li, P. Liu, Y. Zhang, H. Zhang, Y. Tang, *Inorg. Chem. Front.* **2022**, *9*, 4030.
[95] C. Zhang, Y. Huang, H. Zhao, H. Zhang, Z. Ye, P. Liu, Y. Zhang, Y. Tang, *ACS Appl. Nano Mater.* **2021**, *4*, 10645.
[96] F. Payet, C. Bouillet, F. Leroux, C. Leuvrey, P. Rabu, F. Schosseler, C. Taviot-Guého, G. Rogez, *J. Colloid Interface Sci.* **2022**, *607*, 621.
[97] I. W. Hamley, *Small-Angle Scattering: Theory, Instrumentation, Data, and Applications*, Wiley, New York, NY **2021**.
[98] K. Norrish, *Nature* **1954**, *173*, 256.
[99] M. Smalley, *Clay Swelling and Colloid Stability*, CRC Press, Boca Raton, FL **2006**.
[100] T. Sasaki, M. Watanabe, *J. Am. Chem. Soc.* **1998**, *120*, 4682.
[101] Z. Liu, R. Ma, M. Osada, N. Iyi, Y. Ebina, K. Takada, T. Sasaki, *J. Am. Chem. Soc.* **2006**, *128*, 4872.
[102] F. Geng, R. Ma, A. Nakamura, K. Akatsuka, Y. Ebina, Y. Yamauchi, N. Miyamoto, Y. Tateyama, T. Sasaki, *Nat. Commun.* **2013**, *4*, 1632.
[103] Y. Song, N. Iyi, T. Hoshide, T. C. Ozawa, Y. Ebina, R. Ma, N. Miyamoto, T. Sasaki, *Chem. Commun.* **2015**, *51*, 17068.
[104] K. El Rifaii, H. H. Wensink, I. Dozov, T. Bizien, L. J. Michot, J.-C. P. Gabriel, J. Breu, P. Davidson, *Langmuir* **2022**, *38*, 14563.
[105] K. Tamura, T. Sasaki, H. Yamada, H. Nakazawa, *Langmuir* **1999**, *15*, 5509.
[106] T. Sasaki, M. Watanabe, H. Hashizume, H. Yamada, H. Nakazawa, *J. Am. Chem. Soc.* **1996**, *118*, 8329.
[107] K. Fukuda, I. Nakai, Y. Ebina, R. Ma, T. Sasaki, *Inorg. Chem.* **2007**, *46*, 4787.
[108] K. Fukuda, K. Akatsuka, Y. Ebina, R. Ma, K. Takada, I. Nakai, T. Sasaki, *ACS Nano* **2008**, *2*, 1689.
[109] F. Geng, R. Ma, Y. Ebina, Y. Yamauchi, N. Miyamoto, T. Sasaki, *J. Am. Chem. Soc.* **2014**, *136*, 5491.
[110] S. S. Ono, O. Matsuoka, S. Yamamoto, *Microporous Mesoporous Mater.* **2001**, *48*, 103.
[111] T. Sasaki, Y. Ebina, Y. Kitami, M. Watanabe, T. Oikawa, *J. Phys. Chem. B* **2001**, *105*, 6116.
[112] J. L. Schlenker, B. K. Peterson, *J. Appl. Crystallogr.* **1996**, *29*, 178.

[113] G. G. Juttu, R. F. Lobo, *Microporous Mesoporous Mater.* **2000**, *40*, 9.
[114] W. J. Roth, D. L. Dorset, G. J. Kennedy, *Microporous Mesoporous Mater.* **2011**, *142*, 168.
[115] C. Perego, A. de Angelis, P. Pollesel, R. Millini, *Ind. Eng. Chem. Res.* **2021**, *60*, 6379.
[116] T. Maluangnont, K. Matsuba, F. Geng, R. Ma, Y. Yamauchi, T. Sasaki, *Chem. Mater.* **2013**, *25*, 3137.
[117] V. Dudko, S. Rosenfeldt, R. Siegel, J. Senker, M. Matejdes, J. Breu, *Langmuir* **2022**, *38*, 10781.
[118] H. V. Thang, J. Vaculík, J. Prech, M. Kubu, J. Cejka, P. Nachtigall, R. Bulánek, L. S. Grajciar, *Microporous Mesoporous Mater.* **2019**, *282*, 121.
[119] J. Sauer, *Faraday Discuss.* **2016**, *188*, 227.
[120] J. V. Alemán, A. V. Chadwick, J. He, M. Hess, K. Horie, R. G. Jones, P. Kratochvíl, I. Meisel, I. Mita, G. Moad, S. Penczek, *R. F. T. Stepto* **2007**, *79*, 1801.
[121] K. Kalahurska, P. P. Ziemianski, W. J. Roth, B. Gil, *Molecules* **2021**, *26*, 2076.
[122] B. N. Desai, P. M. Barve, *Nature* **1931**, *128*, 907.
[123] L. Qian, H. Zhang, *J. Chem. Technol. Biotechnol.* **2011**, *86*, 172.
[124] J. E. Brydon, H. M. Rice, G. C. Soott, *Can. J. Soil Sci.* **1963**, *43*, 404.
[125] E. S. Tsurko, P. Feicht, F. Nehm, K. Ament, S. Rosenfeldt, I. Pietsch, K. Roschmann, H. Kalo, J. Breu, *Macromolecules* **2017**, *50*, 4344.
[126] M. Röhrl, J. H. Mettke, S. Rosenfeldt, H. Schmalz, U. Mansfeld, R. L. Timmins, C. Habel, J. Breu, F. Durst, *J. Coat. Technol. Res.* **2022**, *19*, 487.
[127] B. Gil, W. J. Roth, W. Makowski, B. Marszalek, D. Majda, Z. Olejniczak, P. Michorczyk, *Catal. Today* **2015**, *243*, 39.
[128] M. Osada, T. Sasaki, *Polym. J.* **2015**, *47*, 89.
[129] T. Nakato, W. Ishitobi, M. Yabuuchi, M. Miyagawa, E. Mouri, Y. Yamauchi, *Langmuir* **2021**, *37*, 7789.
[130] T. Nakato, A. Takahashi, S. Terada, S. Yamaguchi, E. Mouri, M. Shintate, S. Yamamoto, Y. Yamauchi, N. Miyamoto, *Langmuir* **2019**, *35*, 14543.
[131] R. Millini, G. Bellussi, *RSC Catal. Ser.* **2017**, *28*, 1.
[132] E. T. C. Vogt, B. M. Weckhuysen, *Chem. Soc. Rev.* **2015**, *44*, 7342.
[133] K. Ogorzaly, B. Gil, M. Mazur, W. Makowski, W. J. Roth, *Microporous Mesoporous Mater.* **2021**, *324*.
[134] K. Kalahurska, W. Pajerski, A. Kotarba, M. Kubu, Y. Zhang, M. Mazur, J. Prech, G. Jajko, W. Makowski, W. J. Roth, B. Gil, *Catal. Today* **2022**, *390*, 335.
[135] Y. Zhang, M. Kubu, M. Mazur, J. Cejka, *Catal. Today* **2019**, *324*, 135.
[136] A. Li, Y. Zhang, C. J. Heard, K. Golabek, X. Ju, J. Cejka, M. Mazur, *Angew. Chem., Int. Ed.* **2023**, *62*, 202213361.
[137] M. E. Davis, *Chem. Mater.* **2014**, *26*, 239.
[138] J. Grzybek, W. J. Roth, B. Gil, A. Korzeniowska, M. Mazur, J. Cejka, R. E. Morris, *J. Mater. Chem. A* **2019**, *7*, 7701.
[139] M. Hartmann, A. G. Machoke, W. Schwieger, *Chem. Soc. Rev.* **2016**, *45*, 3313.
[140] A. Korzeniowska, J. Grzybek, K. Kalahurska, M. Kubu, W. J. Roth, B. Gil, *Catal. Today* **2020**, *345*, 116.
[141] D. Liu, X. Zhang, A. Bhan, M. Tsapatsis, *Microporous Mesoporous Mater.* **2014**, *200*, 287.
[142] A. Korde, B. Min, Q. Almas, Y. Chiang, S. Nair, C. W. Jones, *ChemCatChem* **2019**, *11*, 4548.
[143] K. Mantri, K. Komura, Y. Kubota, Y. Sugi, *J. Mol. Catal. A: Chem.* **2005**, *236*, 168.
[144] K. Ogorzaly, G. Jajko, K. Wolski, S. Zapotoczny, M. Kubu, W. J. Roth, B. Gil, W. Makowski, *Catal. Today* **2022**, *390*, 272.
[145] Y. Li, G. Zhu, Y. Wang, Y. Chai, C. Liu, *Microporous Mesoporous Mater.* **2021**, *312*, 110790.
[146] W. J. Roth, C. T. Kresge, *Microporous Mesoporous Mater.* **2011**, *144*, 158.
[147] M. Dyballa, D. K. Pappas, E. Borfecchia, P. Beato, U. Olsbye, K. P. Lillerud, B. Arstad, S. Svelle, *Microporous Mesoporous Mater.* **2018**, *265*, 112.
[148] D. Chimene, D. L. Alge, A. K. Gaharwar, *Adv. Mater.* **2015**, *27*, 7261.
[149] D. O'Hare, *Inorganic Intercalation Compounds* (Eds.: D. W. Bruce, D. O'Hare), Inorganic Materials, Wiley, New York, NY **1997**, pp. 172-254.
[150] R. Ma, T. Sasaki, *Acc. Chem. Res.* **2015**, *48*, 136.
[151] T. A. Shifa, F. Wang, Y. Liu, J. He, *Adv. Mater.* **2019**, *31*, 1804828.
[152] A. K. Gaharwar, L. M. Cross, C. W. Peak, K. Gold, J. K. Carrow, A. Brokesh, K. A. Singh, *Adv. Mater.* **2019**, *31*, 1900332.
[153] M. Gobbi, E. Orgiu, P. Samorì, *Adv. Mater.* **2018**, *30*, 1706103.
[154] R. Ma, T. Sasaki, *Adv. Mater.* **2010**, *22*, 5082.

Wieslaw J. Roth is a professor at the Faculty of Chemistry of the Jagiellonian University in Krakow, Poland. He worked at Mobil R&D in Paulsboro and ExxonMobil R&E in Clinton, New Jersey, for 21 years prior to joining the Faculty in 2012. He received the D. W. Breck Award in 1994 for the co-discovery of ordered mesoporous materials, Thomas Alva Edison Award in 2008 for the patent and commercialization of mesoporous materials, and the FEZA Cronsted Awards in 2020, jointly with J. Cejka, for the contributions to the development of layered zeolites.

Maksym Opanasenko received his MSc degree in Chemistry from the Lomonosov Moscow State University. He continued his PhD study at Pisarzhevsky Institute of Physical Chemistry (the National Academy of Sciences of Ukraine) and obtained his PhD degree in porous polymeric and composite materials in 2011. In 2011 Maksym joined the group of Prof. Čejka at Heyrovsky Institute of Physical Chemistry, ASCR. From 2021 Maksym has been holding an Associate Professor position at the Faculty of Science, Charles University in Prague. Currently, he is focused on the design of new nanostructured inorganic and hybrid materials and their application in catalysis.

Michal Mazur is an Assistant Professor and a head of Electron Microscopy Laboratory at the Department of Physical and Macromolecular Chemistry, Charles University, Prague, Czechia. He obtained his PhD in chemistry from Charles University in 2016. Afterward, he held a post-doctoral position at the University of St Andrews, Scotland. Michal has been investigating novel approaches to synthesis of zeolites, focusing on the use of 2D layered precursors and functionalization of zeolites with metal nanoparticles. His main interest is characterization of zeolitic materials by advanced electron microscopy and diffraction techniques.

Barbara Gil is a full Professor and the Head of Zeolite Chemistry Group at the Faculty of Chemistry of the Jagiellonian University. She has specialized in the synthesis and characterization of micro- and mesoporous materials. Her main areas of interest are the classical 3D zeolites and the new class of lamellar 2D zeolites, MOFs and ordered silica mesoporous materials. Her research combines IR spectroscopy with catalysis and drug delivery. She is an expert in quantitative characterization of acidic and redox centers in general and in environmentally important reactions. She is a co-author of over 140 scientific articles.

Jiří Čejka is a professor at the Department of Physical and Macromolecular Chemistry at the Faculty of Science of the Charles University. He obtained his PhD at the Czechoslovak Academy of Sciences in 1988. In 2016 he joined the Faculty of Science where he is leader of the research group focused on the synthesis, characterization and application of zeolites and other porous materials in adsorption and catalysis. He is a principal investigator of projects supported by the Czech Science Foundation and Horizon Europe. He received the FEZA Cronsted Awards in 2020, jointly with W. J. Roth.

Takayoshi Sasaki is a principal investigator of Research Center for Materials Nanoarchitectonics (WPI-MANA) at the National Institute for Materials Science (NIMS) in Japan. He obtained his PhD in chemistry from the University of Tokyo in 1985. Since 1980, he has been working for the National Institute for Research in Inorganic Materials (NIRIM, now NIMS), Japan. In 2009, he was appointed as a NIMS fellow. He has been investigating layered transition metal oxides and hydroxides and their delaminated 2D nanosheets.